https://doi.org/10.5194/egusphere-2023-2432
Preprint. Discussion started: 13 December 2023

Limited effect of the confluence angle and tributary gradient on Alpine confluence morphodynamics under intense sediment loads

Authors:

Théo St. Pierre Ostrander(1) – Corresponding Author

theo.st-pierre-ostrander@uibk.ac.at

Thomé Kraus(2)

Thome.Kraus@student.uibk.ac.at

Bruno Mazzorana(3)

bruno.mazzorana@uach.cl

Johannes Holzner(4)

Johannes.Holzner@provinz.bz.it

Andrea Andreoli(5)

Andrea.Andreoli@unibz.it

Francesco Comiti(6)

Francesco.Comiti@unibz.it

Bernhard Gems(7)

bernhard.gems@uibk.ac.at

(1, 2, 7) University of Innsbruck, Unit of Hydraulic Engineering, Technikerstraße 13a, 6020, Innsbruck, Austria

(3) Universidad Austral de Chile, Faculty of Sciences, Instituto de Ciencias de la Tierra, Edificio Emilio Pugín, Avenida Eduardo Morales Miranda, Campus Isla Teja, Valdivia, Chile

(4, 5, 6) Free University of Bozen-Bolzano, Faculty of Agricultural, Environmental and Food Sciences, Universitätsplatz 5 - piazza Università, 5, 39100, Bozen-Bolzano, Italy

https://doi.org/10.5194/egusphere-2023-2432
Preprint. Discussion started: 13 December 2023

Abstract

Confluences are dynamic morphological nodes in all river networks. In mountain regions, they are influenced by hydraulic and sedimentary processes occurring in steep channels during extreme events in small watersheds. Sediment transport in the tributary channel and aggradation in the confluence can be massive, potentially causing overbank flooding and sedimentation into adjacent settlement areas. Previous works dealing with confluences have been mainly focused on lowland regions, or if focused on mountain areas, the sediment concentrations and channel gradients were largely under-representative of mountain river conditions. The presented work contributes to filling this research gap with 45 experiments using a large-scale physical model. Geometric model parameters, applied grain size distribution, and the considered discharges represent the conditions at 135 confluences in South Tyrol (Italy) and Tyrol (Austria).

The experimental program allowed for a comprehensive analysis of the effects of (i) the confluence angle, (ii) the tributary gradient, (iii) the channel discharges, and (iv) the tributary sediment concentration. Results indicate, in contrast to most research dealing with confluences, that in the presence of intense tributary sediment supply and a small tributary to main channel discharge ratio (0.1), the confluence angle does not have a decisive effect on confluence morphology. Adjustments to the tributary channel gradient yielded the same results. A reoccurring range of depositional geomorphic units was observed where a deposition cone transitioned to a bank-attached bar. The confluence morphology and tributary channel gradient rapidly adjusted, tending towards an equilibrium state to accommodate both water discharges and the sediment load from the tributary. Statistical analyses demonstrated that confluence morphology was controlled by the combined channel discharge and the depositional or erosional extents by the sediment concentration. Applying the conclusions drawn from lowland confluence dynamics could misrepresent depositional and erosional patterns and the related flood hazard at mountain river confluences.

Keywords: Confluence Morphology; Fluvial Hazard; Steep Tributary; Bedload; Physical Scale Model; Mountain Rivers

https://doi.org/10.5194/egusphere-2023-2432
Preprint. Discussion started: 13 December 2023

1 Introduction

River confluences are important features of all river systems and are sites of significant hydraulic and morphological change (Benda et al., 2004). They are characterized by converging flow paths that produce complex 3-dimensional hydraulics that influence the local morphology, and fluvial dynamics (Best, 1987; 1988; Rhoads & Kenworthy, 1995; Benda et al., 2004; Boyer et al., 2006; Ferguson & Hoey, 2008; Guillén-Ludeña et al., 2015; Guillén-Ludeña et al., 2017). In developed areas, confluences form critical junctions as the hydraulic geometries and sediment loads from each channel must be accommodated to avoid overbank flooding and sedimentation (Gems et al., 2014; Liu et al., 2015; Kammerlander et al., 2016; Sturm et al., 2018). The importance of these junctions has garnered much research interest, which has illuminated many characteristics of the hydro-morphodynamic interactions, and the major controls on the flow structure occurring at lowland river confluences (Mosley, 1976; Best, 1987; 1988; Biron et al., 1993; Rhoads & Kenworthy, 1995; Bradbrook et al., 1998; De Serres et al., 1999; Benda et al., 2004; Boyer et al., 2006; Wang et al., 2007; Liu et al., 2015). Best (1987; 1988) built upon the seminal work of Mosley (1976) in his identification of hydraulic and morphologic zones occurring at confluences. The typically occurring hydraulic zones are flow separation, flow stagnation, flow deflection, maximum velocity, shear layers, and recovery zone. These zones influence sediment transport pathways through the confluence and the resulting morphological elements of confluences: avalanche faces at the mouth of each confluent channel, a deep central scour hole, and a bar in the separation zone. Best (1988) concluded that the controlling variables as to the location, orientation, and size of these morphologic zones are the confluence angle and the discharge ratio $Q_r = Q_t/Q_m$ which is the ratio of the tributary (Q_t) and the main channel (Q_m) discharges.

Confluences in mountain regions have not received the same attention as those in lowland areas, which is surprising given the hazard potential associated with large volumes of coarse sediment entering these critical junctions (Aulitzky, 1989). Differentiation between mountain and lowland confluences can be described by (i) supercritical or transitioning flow conditions in the tributary channel, (ii) bed surface armoring due to the size heterogeneity of the tributary sediment load or non-erodible conditions in the tributary channel as a result of hazard protection measures, (iii) high sediment concentrations during flooding events and (iv) highly variable discharges and sediment transport rates (Aulitzky, 1980; 1989; Meunier, 1991; Roca et al., 2009; Guillén-Ludeña et al., 2017). Topographic confinement can amplify confluence effects, whereas

https://doi.org/10.5194/egusphere-2023-2432
Preprint. Discussion started: 13 December 2023

in lowland regions with wide valley floors and broad terraces, deposition cones or fans can be isolated from the main channel (Benda et al., 2004). A sudden introduction of sediment from steep tributaries can trigger numerous types of morphological changes (Benda et al., 2004), as tributaries of confined channel confluences can be particularly disruptive (Rice, 1998).

Detailed records of flash flooding associated with intense sediment transport in Tyrol (Austria) show that these events are a persistent hazard (Embleton-Hamann, 1997; Rom et al., 2023). In the Alps, hazardous events can impact high-population-density valleys. Increased or shifting flooding patterns (Blöschl et al., 2017; Löschner et al., 2017; Blöschl et al., 2020; Hanus et al., 2021) and enhanced sediment availability (Knight & Harrison, 2009; Stoffel et al., 2012; Gems et al., 2020) as a consequence of climate change (Keiler et al., 2010) not only threatens new infrastructure but challenges previously installed mitigation measures. Relevant hazard events are typically triggered by localized short-duration-high intensity convective storms occurring in small watersheds, which do not significantly affect main channel discharge and bedload transport (Gems et al., 2014; Hübl & Moser, 2006; Prenner et al., 2019; Stoffel, 2010). The narrow, steep tributary provides the sediment load to the main channel, which supplies the dominant flow discharge (Miller, 1958; Guillén-Ludeña et al., 2017).

Most of the work that has been done on mountain river confluences has been focused on conditions that do not typically generate hazardous events, mainly under-representations of gradients and sediment concentrations (Roca et al., 2009; Leite Ribeiro et al., 2012a; Leite Ribeiro et al., 2012b; Guillén-Ludeña et al., 2015; Guillén-Ludeña et al., 2017). Complicating the conclusions drawn regarding confluence morphodynamics, St. Pierre Ostrander et al. (2023) established, from a set of 15 experiments, that confluences of mountain rivers are influenced by factors other than the confluence angle and the discharge ratio. They held the confluence angle and discharge ratio constant, only adjusting discharges and tributary sediment concentration. They observed a range of morphologies with specific geomorphic units, a deposition cone, a transitional morphology, a bank-attached bar, and a scour hole. They used unit stream power to predict and associate confluence zone morphology with hydraulic conditions. However, they were limited in their conclusions and recommended further experiments considering additional geometries as their experimental program was not sufficiently comprehensive, restricting the reach of their findings. The channel geometry was unchanged throughout the experimental program, and morphological assessment

https://doi.org/10.5194/egusphere-2023-2432
Preprint. Discussion started: 13 December 2023

lacked statistical evaluation and grain size analysis. This paper builds upon these experimental results with an additional 30 experiments considering geometric modifications. In addition to investigating the effects of the channel discharge and sediment concentration, adjustments to the confluence angle and the tributary gradient provide a more comprehensive data analysis of fluvial hazard processes and the resulting morphologies of mountain river confluences. Evaluating morphological patterns and extents was done qualitatively with DEMs of Difference (DoD) created from laser sans, quantitatively from the extents of geomorphic units, depositional and erosional values, and volumetric grain samples, and statistically. Statistical analysis determined which of the introduced factors significantly impacted the response variables controlling the morphodynamic development of mountain river confluences. Results from the 45 experiments tested the following hypotheses:

1. Adjustments to the confluence angle and the tributary gradient do not significantly impact confluence morphology and the development of specific geomorphic units (hypothesis 1).
2. Of the introduced factors, the sediment concentration and channel discharge exert the most control over depositional and erosional patterns (hypothesis 2).

2 Model and Methods

2.1 Experimental program

The physical scale model (Fig. 1) was constructed to represent a typical confluence in the regions of South Tyrol (Italy) and Tyrol (Austria). The experimental setup served as a generic configuration to reproduce the main hydrodynamic and sedimentary processes occurring at mountain river confluences while gaining insights into the dominant control variables. Experimental modeling uses and builds upon the configuration, calibration, and experiments (1-15) carried out by St. Pierre Ostrander et al. (2023), but with an additional tributary gradient and confluence angle. Model dimensions, discharges, and the grain size distribution of the input material and the main channel bed were based on an analysis of 135 confluences and 65 volume and line samples in the study region (St. Pierre Ostrander et al., 2023). The main channel had a mobile bed, allowing for 0.2 m of erosion and the tributary channel had a fixed bed. Tributary bed roughness was created using an adhesive to apply a layer of quartz sand to the bed. Channel roughness was established through hydraulic manuals (Chow, 1959) and previous calibration work (St. Pierre Ostrander et al., 2023). A grain size distribution curve and the gradation coefficient (σ) of both the mobile bed and the input material are included in Fig. 1. The physical model was adjustable, except for the width of the tributary (0.2 m) and the lengths of the channels (5.0 m and 9.0 m for the tributary and main channel, respectively). Discharge to each channel was supplied by a separate pump controlled by an electronic flow measurement device. The discharge ratio was fixed at 0.1 for all experiments. The tributary sediment discharge was always proportional to the clear water discharge; an increase in tributary discharge meant an increase in both clear water and sediment discharges. The main channel flow was exclusively clear water to replicate typical events that produce massive aggradation at confluences (Hübl & Moser, 2006; Stoffel, 2010; Gems et al., 2014; Prenner et al., 2019). Scaling was done according to Froude similarity; transferring model dimensions to nature allows a scale factor range of 20-40. The scale is determined by the width of the tributary at the confluence relative to the width of the tributary in the physical model and was referred to as the specific scale (St. Pierre Ostrander et al., 2023).

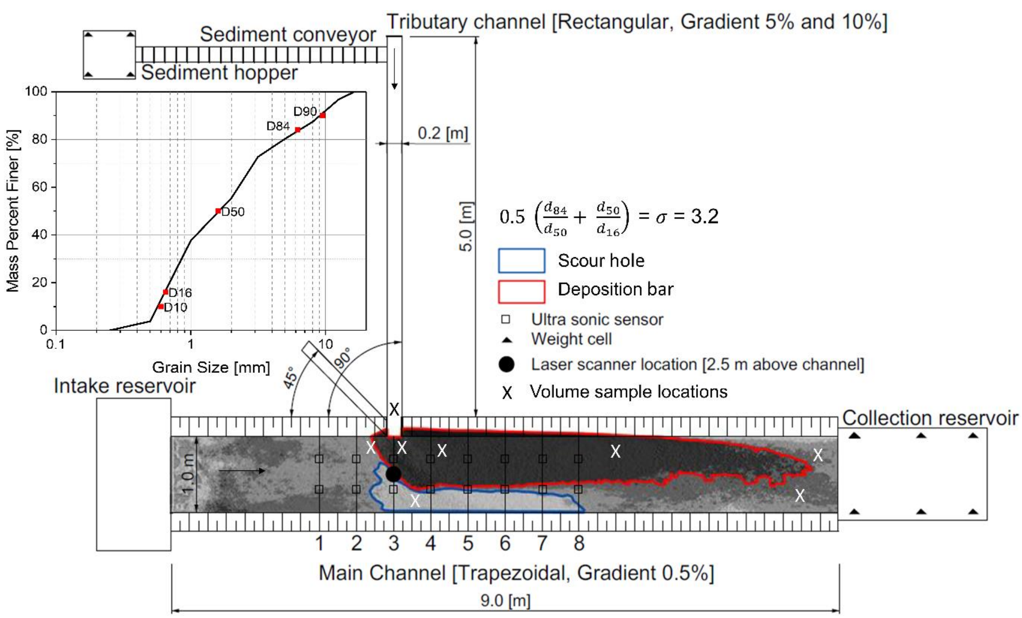

Figure 1 Overview of the physical model showing the location of measurement devices, volume sample locations, the gradation coefficient (σ), the grain size distribution of the sediment supplied to the tributary channel and the mobile bed in the main channel, and an example of the scour hole and the deposition bar.

https://doi.org/10.5194/egusphere-2023-2432
Preprint. Discussion started: 13 December 2023

Experiments (Table 1) allowed for the same 5 steady-state discharge combinations to be tested with different tributary gradients, confluence angles, and sediment concentrations, which were based on the bulk density of the input material. The morphological development of the confluence zone for each geometric setup was evaluated by creating DEMs of Difference (DoD) (*ESRI ArcGIS Desktop, Release 10.8.2*) from laser scans (*Faro Focus 3D, Trimble X7*) taken before and after an experiment. The initial bathymetry was the reference, which was established by running a low discharge of 15 l s^{-1} in the main channel for 5 hours to create a more natural river bed. The post-run bathymetry was the comparison (St. Pierre Ostrander et al., 2023). Morphological evaluation was done by assessing specific zones and overall changes occurring in the channel. The deposition bar and scour hole were delineated by deposition or erosion above or below 0.01 m (Fig. 1). Main channel deposition and erosion areas and volumes reflect morphological change occurring throughout the entire channel above or below the initial bathymetry.

Based on historical records, the scaled experiment duration was 20 minutes and started when sediment entered the tributary channel. The only alterations between the experimental groups were changing the tributary gradient and the confluence angle. Experiments 1-15 had a 10 % tributary gradient, a 90° confluence angle, and a main channel gradient of 0.5 %. Experiments 16-30 had the same geometric configuration except with a 5 % tributary gradient. Experiments 31-45 had a 10 % tributary gradient and a 45° confluence angle; the main channel gradient remained unchanged. The respective dimensions were chosen as they are the most representative of the study region (St. Pierre Ostrander et al., 2023). DEMs of Difference were created from the DoDs of experiments with identical input conditions, i.e., discharge and sediment supply rate, allowing for a visual assessment of morphological differences based on geometric changes alone. For example, experiments 1 and 16 had equal discharges and sediment concentrations; the only change was the tributary gradient, and experiments 1 and 31 had the same discharges, sediment concentrations, and gradients, but the confluence angle was changed. The 10 % gradient tributary with a 90° confluence angle was used as the reference as both geometric configurations are comparable, and changes in gradient and confluence angle could be accurately assessed.

https://doi.org/10.5194/egusphere-2023-2432
Preprint. Discussion started: 13 December 2023

Table 1 Experiment target and actual discharges and sediment concentration, and tributary sediment supply rate. Experiment 30 was not able to be completed as the deposition in the tributary caused overtopping of the channel.

	EXP [-]	Q_m Target [l s^{-1}]	Q_m Actual [l s^{-1}]	Q_t Target [l s^{-1}]	Q_t Actual [l s^{-1}]	Sed. conc. Target [%]	Sed. conc. Actual [%]	Sed. supply rate [kg min^{-1}]
10% Tributary Gradient 90° Confluence Angle	1	15.0	15.3	1.5	1.5	5.0	*	7.6
	2	45.0	45.6	4.5	4.3	5.0	*	22.9
	3	75.0	75.5	7.5	7.4	5.0	5.7	43.5
	4	105.0	104.5	10.5	10.6	5.0	4.9	53.4
	5	135.0	135.4	13.5	13.4	5.0	5.2	68.7
	6	15.0	15.1	1.5	1.5	7.5	7.6	11.4
	7	45.0	46.1	4.5	4.4	7.5	7.5	34.3
	8	75.0	75.3	7.5	7.5	7.5	7.3	57.2
	9	105.0	105.1	10.5	10.5	7.5	7.6	80.1
	10	135.0	134.7	13.5	13.4	7.5	7.5	103.0
	11	15.0	14.8	1.5	1.5	10.0	*	15.3
	12	45.0	44.9	4.5	4.6	10.0	10.1	45.8
	13	75.0	76.1	7.5	7.6	10.0	10.3	76.3
	14	105.0	105.7	10.5	10.4	10.0	10.4	106.8
	15	135.0	135.4	13.5	13.6	10.0	*	137.3
5% Tributary Gradient 90° Confluence Angle	16	15.0	15.9	1.5	1.4	5.0	*	7.6
	17	45.0	46.0	4.5	4.5	5.0	5.1	22.9
	18	75.0	75.9	7.5	7.6	5.0	5.0	43.5
	19	105.0	104.4	10.5	10.4	5.0	5.1	53.4
	20	135.0	134.7	13.5	13.5	5.0	5.2	68.7
	21	15.0	15.5	1.5	1.4	7.5	*	11.4
	22	45.0	46.7	4.5	4.3	7.5	7.8	34.3
	23	75.0	74.9	7.5	7.5	7.5	7.5	57.2
	24	105.0	105.5	10.5	10.4	7.5	7.5	80.1
	25	135.0	134.6	13.5	13.4	7.5	7.9	103.0
	26	15.0	15.1	1.5	1.6	10.0	9.6	15.3
	27	45.0	43.5	4.5	4.4	10.0	10.2	45.8
	28	75.0	75.0	7.5	7.6	10.0	10.1	76.3
	29	105.0	105.9	10.5	10.5	10.0	10.1	106.8
	30	135.0	-	13.5	-	-	-	-
10% Tributary Gradient 45° Confluence Angle	31	15.0	14.6	1.5	1.6	5.0	*	7.6
	32	45.0	45.0	4.5	4.3	5.0	5.2	22.9
	33	75.0	75.8	7.5	7.7	5.0	4.9	43.5
	34	105.0	105.1	10.5	10.5	5.0	5.0	53.4
	35	135.0	134.9	13.5	13.5	5.0	5.0	68.7
	36	15.0	15.0	1.5	1.5	7.5	*	11.4
	37	45.0	45.6	4.5	4.5	7.5	7.6	34.3
	38	75.0	75.2	7.5	7.5	7.5	7.7	57.2
	39	105.0	106.1	10.5	10.5	7.5	7.6	80.1
	40	135.0	135.6	13.5	13.4	7.5	8.0	103.0
	41	15.0	14.8	1.5	1.4	10.0	10.4	15.3
	42	45.0	44.9	4.5	4.4	10.0	10.1	45.8
	43	75.0	75.5	7.5	7.6	10.0	9.9	76.3
	44	105.0	105.8	10.5	10.4	10.0	9.3	106.8
	45	135.0	135.0	13.5	13.5	10.0	*	137.3

*indicates that the sediment was delivered manually or with manual assistance as the dosing machine could not dose very low or high rates of sediment into the tributary channel

https://doi.org/10.5194/egusphere-2023-2432
Preprint. Discussion started: 13 December 2023

2.2 Statistical analysis

A statistical analysis of the various introduced factors and their effects on the response variables (Table 2) was done using the software package *OriginPro (v.2023, OriginLab Corp.)* (Stevenson, 2011; Baranovskiy, 2019). The chosen response variables (Table 2), captured either depositional or erosional features, and allowed for a nuanced investigation into the subtle variations that were not able to be qualitatively assessed. The combined discharge was used as a factor since the morphological development of the confluence occurred downstream of the tributary. The confidence interval for all tests was 95 %. A significant result occurred when the p-value, calculated from the test statistic of the applied test, was less than 0.05. A p-value less than 0.05 allowed for rejecting the null hypothesis, which was the factor that did not significantly impact the response variable. If rejected, further pairwise post hoc tests were conducted to determine the decisive factors influencing confluence morphology.

Table 2 Factors and response variables that control and define confluence morphology

Factor	Unit	Response Variable	Unit
Sediment concentration (5, 7.5, 10)	%	Main channel deposition area and volume	m^2, m^3
Combined discharge (16.5, 49.5, 82.5, 115.5, 148.5)	$l\ s^{-1}$	Main channel erosion area and volume	m^2, m^3
Confluence angle (90, 45)	°	Deposition bar area	m^2
Tributary gradient (10, 5)	%	Deposition bar length	m
		Deposition bar width	m
		Scour area	m^2
		Scour length	m
		Scour width	m
		Maximum depths scour and deposition	m

The sequence of operations in Fig. 2 shows the chosen tests, which allowed for planned comparisons (Ruxton & Beauchamp, 2008). The relevant data sets were examined to ensure that the correct statistical and pairwise post hoc tests were applied (Welch, 1947; Massey, 1951; Dunn, 1964; Maxwell & Delaney, 2004; Steinskog et al., 2007; Sawyer, 2009; McKnight et al., 2010; Moder, 2010; Witte & Witte, 2017; Delacre et al., 2019). Determining which tests were applied for a specific factor was based on the sample coming from a population of a specific distribution, then verifying heterogeneity or homogeneity of variances. This established the following hypothesis and subsequent post hoc tests, if applicable. Not all the tests were

https://doi.org/10.5194/egusphere-2023-2432
Preprint. Discussion started: 13 December 2023

used but were established in case of varying distributions and homogeneity or heterogeneity of variances. Data was grouped by aggregating individual observations for a specific factor. For example, the deposition bar area in response to sediment concentration would have 3 groups, a mean area for each of the 3 tested sediment concentrations; for the confluence angle, the bar area can only have 2 mean values 1 from each angle, so there are only 2 groups.

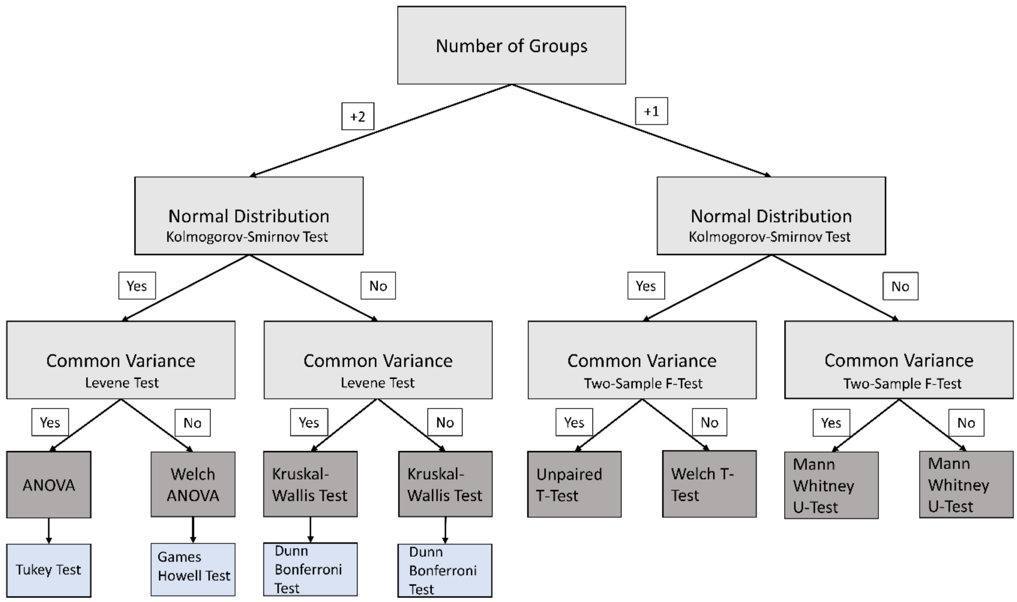

Figure 2 Workflow for assessing the impacts of factors with associated tests based on the distributions and variances of the examined groups.

2.3 Volumetric grain sampling

Volume samples were taken after an experiment with sample locations corresponding to both morphologic and hydraulic zones occurring in the channel. In total 8 samples were taken for each experiment. The sampled volume was 0.002 m^3 with an average sample mass of 3.3 kg which was taken by inserting a cylinder (0.16 m diameter and 0.1 m height) into the channel bed or depositional form. The sampled mass is within the guidelines of Bunte and Abt (2001) (Eq. 1), a larger volume would not be suitable to accurately represent small areas of deposition or erosion as material outside of the area of interest would be

https://doi.org/10.5194/egusphere-2023-2432
Preprint. Discussion started: 13 December 2023

additionally captured. The samples were dried after collection and before the sieving analysis. During sieving the material was separated into 10 fractions based on the mesh size of each sieve. The masses of each fraction were determined and plotted as grain size distribution curves. This grain analysis provided insights into the hydraulic influence on the various zones.

$$\text{Mass}_{\text{sample}}\,(\text{kg}) = 0.1 * 10^{b} * \rho_s * D_{max}^3 \qquad \text{(Equation 1)}$$

Where D_{max} is the maximum grain size, ρ_s is grain density, b is the accuracy level, high (b = 5), medium (b = 4), low (b = 3)

3 Results

3.1 Development and evolution of confluence morphology

Table 3 associates the three depositional geomorphic units consistently observed for all channel configurations and sediment concentrations with unit stream power. They were (i) deposition cone (Fig. 3a to 3c, Appendix 1a to 9a, (ii) transitional morphology (Fig. 3d to 3f, Appendix 1b to 9b), and the (iii) attached-to-the-left-channel-wall separation zone bar (Fig. 3g to 3i, Appendix 1c-e to 9c-e). The scour hole, an erosional geomorphic unit (Fig. 3), was apparent in all experiments (Appendix 1-9) on the right bank opposite the tributary. The deposition cone was characterized by deposition upstream of the confluence in the main channel, a compact longitudinal extent, and steep gradients in both upstream and downstream directions. Cone formation resulted from insufficient transport capacity of the main channel flow and a sustained and abundant sediment supply from the tributary channel. Deposition cones formed for all configurations and sediment concentrations when the discharge was 15 l s^{-1} and 1.5 l s^{-1} in the main and tributary channels, respectively. The transitional morphology occurring in the hydraulic separation zone derived from increased discharge and subsequent unit stream power where experimental discharges of 45 l s^{-1} in the main and 4.5 l s^{-1} in the tributary had nearly forced the bar over to the left bank, but morphological aspects of the deposition cone remained. Discharges and related unit stream power above 45 l s^{-1} in the main and 4.5 l s^{-1} in the tributary allowed for the development of an attached-to-the-left-channel-wall separation zone bar. The bar had the greatest longitudinal extent and the largest storage capacity for

https://doi.org/10.5194/egusphere-2023-2432
Preprint. Discussion started: 13 December 2023

tributary transported sediment. Once the separation zone bar was fully developed, the hydraulic separation zone was filled with deposited sediment and flanked by the maximum velocity zone on the right, which has been observed at lowland confluences with subcritical flows and larger discharge ratios (Best, 1988; Biron et al., 1993; De Serres et al., 1999).

Table 3 Geomorphic units associated with unit stream power (ω), the subscript "*m*" denotes the main channel with the associated gradient and discharge while "*t*" denotes the tributary conditions.

		90° Confluence Angle				45° Confluence Angle	
Experiments	**Geomorphic Unit**	$\omega_{m\_0.5\%}$	$\omega_{t\_10\%}$	$\omega_{m\_0.5\%}$	$\omega_{t\_5\%}$	$\omega_{m\_0.5\%}$	$\omega_{t\_10\%}$
[-]	[-]	[W m^{-2}]	[W m^{-2}]	[W m^{-2}]	[W m^{-2}]	[W m^{-2}]	[W m^{-2}]
1, 16, 31	Deposition cone	0.8	7.5	0.8	3.4	0.7	7.8
2, 17, 32	Transitional	2.2	21.3	2.3	11	2.2	21.2
3, 18, 33	Attached-to-channel bar	3.7	36.4	3.7	18.6	3.7	37.6
4, 19, 34	Attached-to-channel bar	5.1	51.9	5.1	25.6	5.2	51.3
5, 20, 35	Attached-to-channel bar	6.6	65.9	6.6	33.2	6.7	66.1
6, 21, 36	Deposition cone	0.7	7.2	0.8	3.5	0.7	7.5
7, 22, 37	Transitional	2.3	21.7	2.3	10.6	2.2	21.8
8, 23, 38	Attached-to-channel bar	3.7	36.6	3.7	18.3	3.7	36.8
9, 24, 39	Attached-to-channel bar	5.2	51.4	5.2	25.6	5.2	51.4
10, 25, 40	Attached-to-channel bar	6.6	65.8	6.6	32.9	6.7	65.7
11, 26, 41	Deposition cone	0.7	7.4	0.7	3.8	0.7	7.0
12, 27, 42	Transitional	2.2	22.4	2.1	10.9	2.2	21.4
13, 28, 43	Attached-to-channel bar	3.7	37.5	3.7	18.7	3.7	37.4
14, 29, 44	Attached-to-channel bar	5.2	51.2	5.2	25.7	5.2	51.1
15, 45	Attached-to-channel bar	6.6	66.6	-	-	6.6	66.1

The scour hole was created hydraulically by the extent of the separation zone forcing the confluent streams to a smaller area, and physically by channel constriction resulting from depositional patterns reducing the area in which the confluent flows may travel (Guillén-Ludeña et al., 2015; St. Pierre Ostrander et al., 2023), thereby increasing flow velocities (Rhoads and Kenworthy, 1995) and transport capacities. Additionally, the absence of avalanche faces inhibits the development of lee-side flow separation cells (Roy & Bergeron, 1990), which segregates sediment around the confluence instead of through it. Field observation of a gravel-bed confluence showed that tracked particles from both channels converge towards the scour hole with no noticeable segregation (Roy & Bergeron,1990). As the hydraulic separation zone filled with sediment, the spatial extent of the scour hole increased. The system tended towards an equilibrium state where sediment was transported through the scour hole, as this was the only available pathway through the confluence. The

https://doi.org/10.5194/egusphere-2023-2432
Preprint. Discussion started: 13 December 2023

size and depth of the scour hole were greatest at lower sediment concentrations, given the same discharge. There was less sediment to be transported and potentially deposited in the scour hole, and the transport capacity of the main channel was not yet exhausted.

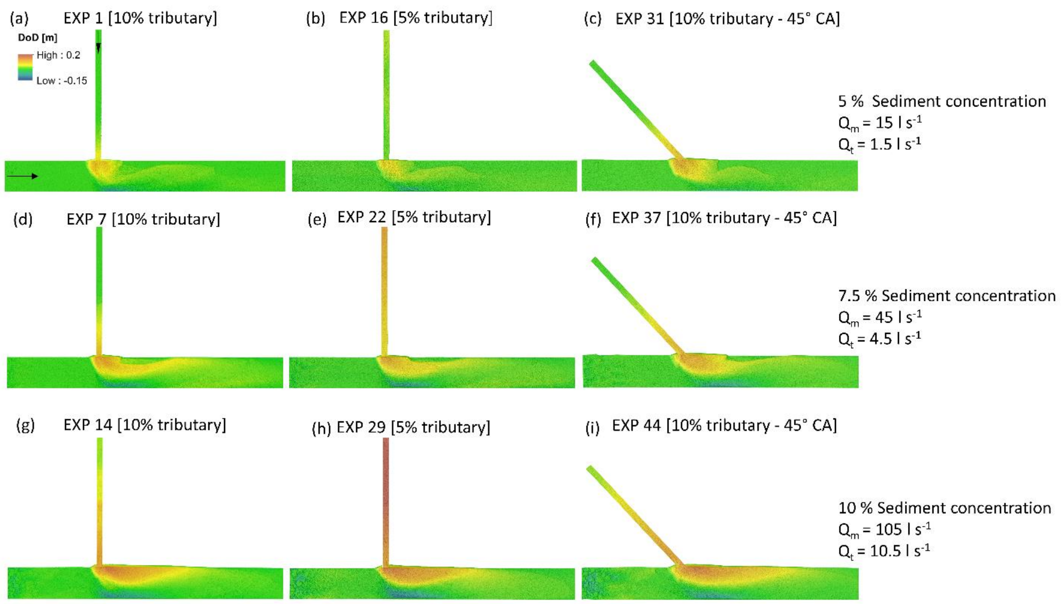

Figure 3 Deposition cone (a-c), transitional (d-f), and attached-to-channel-wall separation zone bar (g-i) geomorphic units with the scour hole on the right, opposite the tributary for all sediment concentrations, confluence angles (CA), and tributary gradients.

3.2 Effects of the tributary gradient

Figure 4 shows the DoDs produced by subtracting the DoDs from experiments 16-30, with a 5 % tributary gradient from experiments 1-15, with a 10 % tributary gradient. The same general morphological patterns consistently occurred regardless of the imposed geometric change. Intense bedload transport in the tributary provided an abundance of sediment to the confluence. The reduced velocity and subsequent transport capacity from the decrease in gradient did not greatly impact the morphological development of the confluence, relative to the depositional forms observed when the gradient was 10 %. This trend could be associated with the unit stream power of the main channel since the same patterns were observed for

https://doi.org/10.5194/egusphere-2023-2432
Preprint. Discussion started: 13 December 2023

all sediment concentrations. As described by Guillén-Ludeña et al. (2017), the main channel supplies the dominant flow at mountain river confluences, if the flow is unchanged then similar development occurs. Main channel unit stream power was consistent for all comparable experiments, the tributary unit stream power was approximately halved when the channel gradient was reduced to 5 % (Table 3).

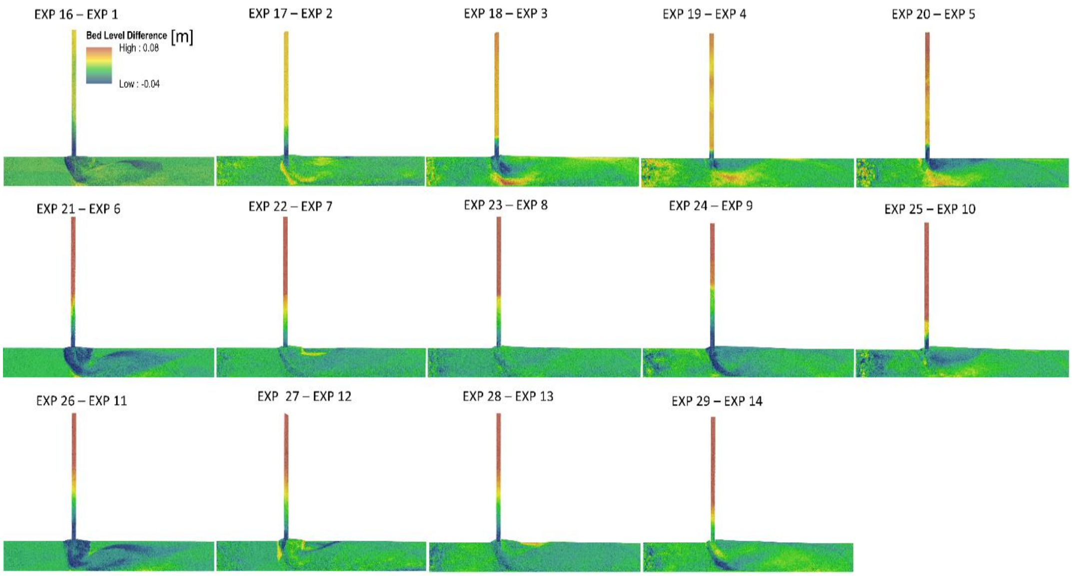

Figure 4 DoDs created by subtracting the DoDs from experiments with a 5 % tributary gradient (16-29) from the DoDs with a 10 % tributary gradient (1-14) supporting a qualitative representation of morphological differences occurring between tributary gradients.

Figure 5 shows the depositional and erosional characteristics of experiments 1-30 excluding the tributary channel. A visual inspection of Fig. 5 does not show a clear trend in differences in depositional or erosional characteristics between gradients. What trend could be inferred is most apparent when comparing the first 5 experiments for each geometry group. Depositional patterns (Fig. 5a, 5c, and 5e) were greater for experiments 16-20 than for experiments 1-5, while erosional patterns were greater for experiments 1-5 than for 16-20 (Fig. 5b, 5d, and 5f). Reducing the tributary channel gradient reduced the velocity of the tributary flow, limiting its contribution to main channel erosion. When the tributary gradient was 10 %, there was

https://doi.org/10.5194/egusphere-2023-2432
Preprint. Discussion started: 13 December 2023

greater penetration of the tributary flow into the main channel and a local increase in transport capacity, creating a larger and deeper scour hole and enhanced conveyance of sediment through the confluence.

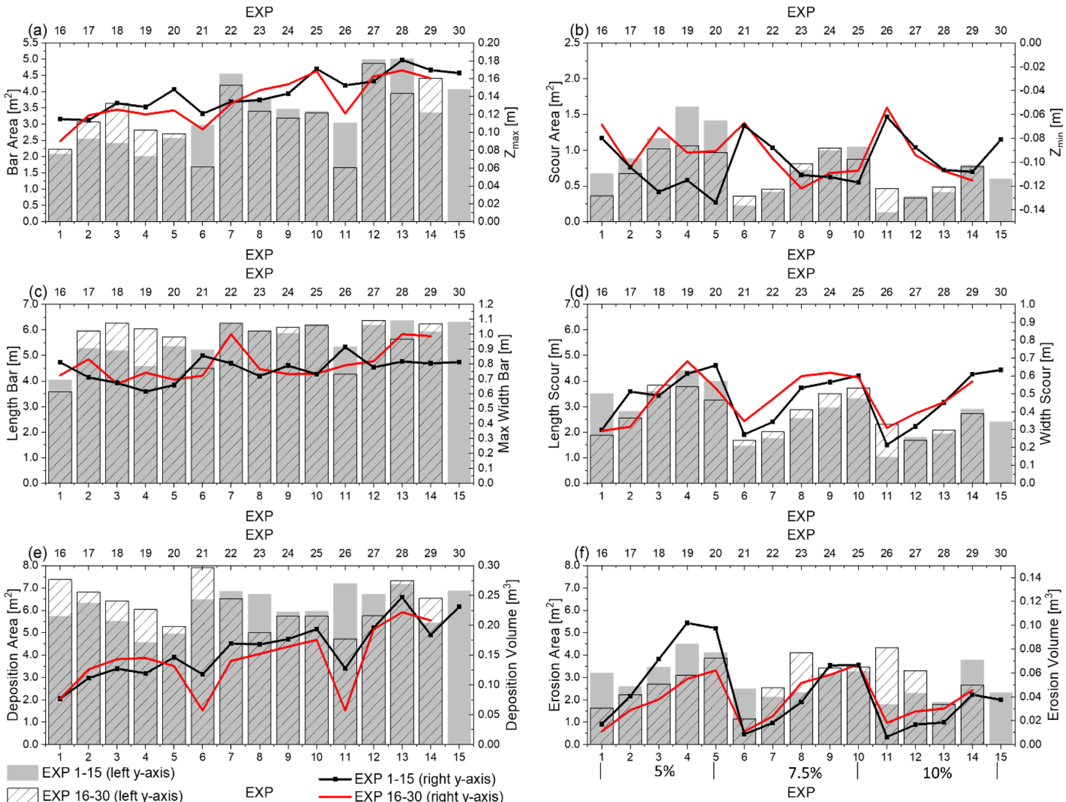

EXP [10% tributary gradient, 90° confluence angle]	EXP [5% tributary gradient, 90° Confluence angle]	Q_m	Q_t
[-]	[-]	[l s^{-1}]	[l s^{-1}]
1, 6, 11	16, 21, 26	15	1.5
2, 7, 12	17, 22, 27	45	4.5
3, 8, 13	18, 23, 28	75	7.5
4, 9, 14	19, 24, 29	105	10.5
5, 10, 15	20, 25, 30	135	13.5

Figure 5 A comparison of morphological attributes across experiments with a 5 % and 10 % tributary gradient, sediment concentration groups are shown in panel f. Deposition bar and scour areas (a, b) are delineated by deposition or erosion above or below 0.01m, respectively. The width and length values represent the maximum measured width or length (c, d), while main channel deposition and erosion areas (e, f) represent all deposition and erosion in the main channel.

https://doi.org/10.5194/egusphere-2023-2432
Preprint. Discussion started: 13 December 2023

Figure 6 shows the gradients of the deposited sediment relative to the initial tributary channel gradient, and deposition volumes in the tributary channel for experiments 1-30. Adjustments to the tributary gradient changed the depositional mechanisms in the tributary channel, characterized by either an increase or decrease in the gradient of the deposited material in the tributary channel, relative to the initial gradient. When the initial gradient was 10 %, the transport capacity of the main channel was the limiting factor for sediment moving through the confluence. This led to a regressive aggradation of sediment, starting at the junction, which decreased the gradient of the tributary channel. Conversely, when the initial tributary channel gradient was 5 %, the resulting decrease in velocity saturated the transport capacity of the tributary channel. Consequently, the depositional patterns switched, and intense progressive deposition occurred starting at the upstream boundary of the tributary channel which increased the gradient of the channel.

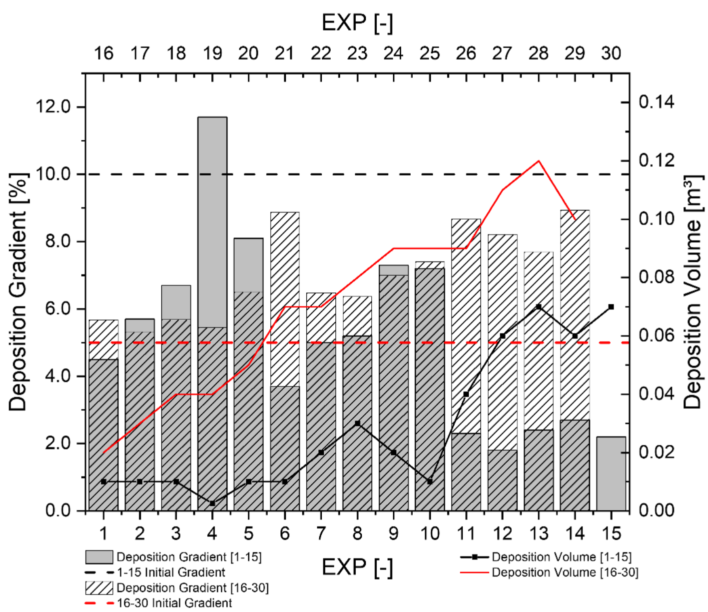

Figure 6 Gradients and volumes of deposited sediment in the tributary channel experiments 1-30.

https://doi.org/10.5194/egusphere-2023-2432
Preprint. Discussion started: 13 December 2023

3.3 Effects of the confluence angle

Figure 7 shows the DoD plots created by subtracting the DoDs produced from experiments with a 45° confluence angle from the DoDs with a 90° confluence angle. The tributary channels with a 45° confluence angle were extracted and referenced to the 90° tributary channels allowing for DoD comparisons. A visual inspection of confluence zone morphology does not reveal drastic changes between confluence angle experiments. Small regions of morphological change are apparent, mainly increased deposition downstream of the junction corner and a generally shallower scour hole when the confluence angle was 45°.

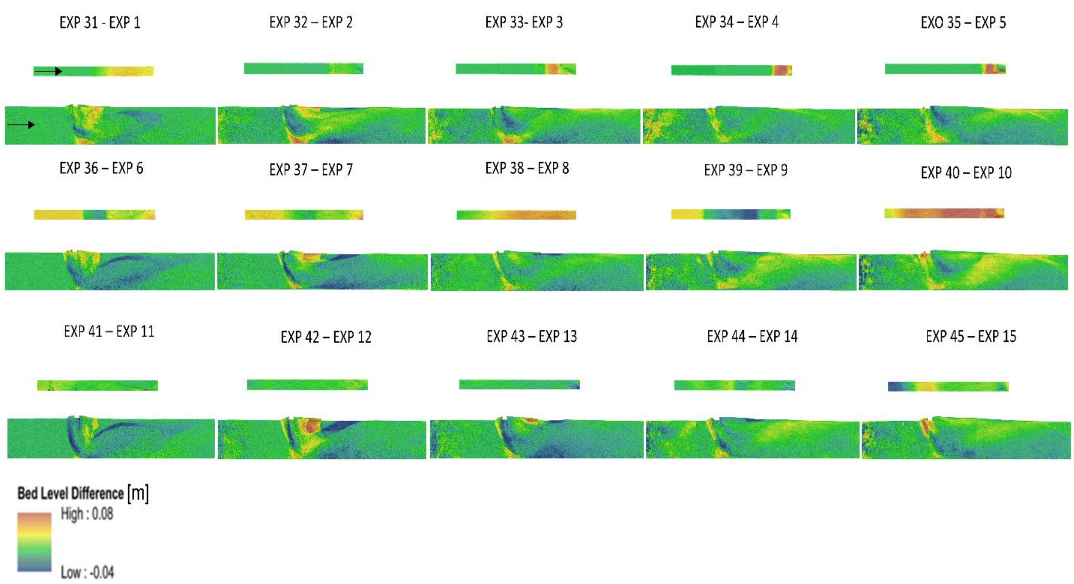

Figure 7 DoDs created by subtracting the DoDs from experiments with a 45° confluence angle (31-45) from the DoDs with a 90° confluence angle (1-15) supporting a qualitative representation of morphological changes occurring between confluence angles.

Figure 8 shows subtle morphological differences with noticeable trends of scour characteristics, while depositional characteristics do not exhibit standout trends upon visual assessment. Both the length and area of the scour hole tended to be greater for experiments 31-45, with a 45° confluence angle (Fig. 8b and

https://doi.org/10.5194/egusphere-2023-2432
Preprint. Discussion started: 13 December 2023

8d). However, the depth of scour and width of the scour was generally greater for experiments 1-15, with a 90° confluence angle. For both confluence angle experiment groups, a clear trend of increasing scour area, length of scour, and erosion area occurred within each sediment concentration group, increasing in response to discharge. Assessing the impact of confluence angle adjustments on depositional attributes requires a statistical approach to reveal any nuanced relationships occurring within the channel.

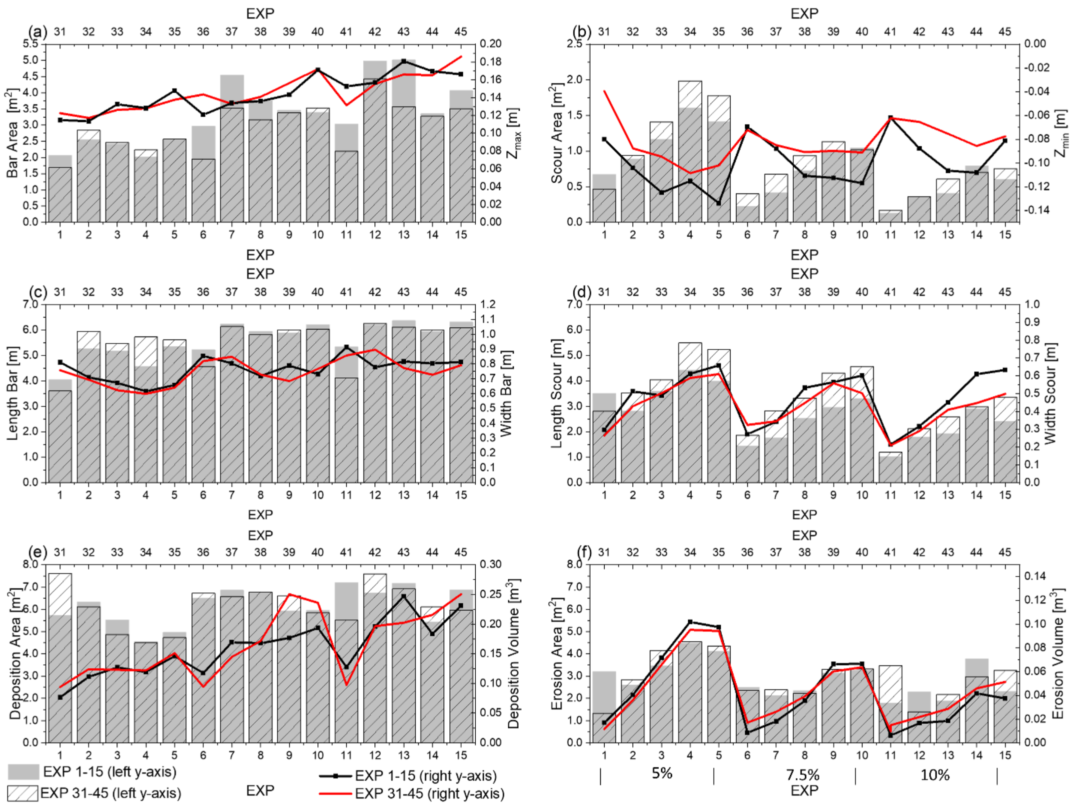

EXP [10% tributary gradient, 90° confluence angle]	EXP [10 % tributary gradient, 45° Confluence angle]	Q_m	Q_t
[-]	[-]	[l s⁻¹]	[l s⁻¹]
1, 6, 11	31, 36, 41	15	1.5
2, 7, 12	32, 37, 42	45	4.5
3, 8, 13	33, 38, 43	75	7.5
4, 9, 14	34, 39, 44	105	10.5
5, 10, 15	35, 40, 45	135	13.5

Figure 8 Comparison of morphological attributes across experiments with a 45° confluence angle and experiments with a 90° confluence angle. Deposition bar and scour areas (a, b) are delineated by deposition or erosion above or below 0.01m, respectively. The width and length values represent the maximum

https://doi.org/10.5194/egusphere-2023-2432
Preprint. Discussion started: 13 December 2023

measured width or length (c, d), while main channel deposition and erosion areas (e, f) represent all deposition and erosion in the main channel.

Figure 9 illustrates that variations in tributary depositional properties occurred despite maintaining a consistent tributary gradient across the experimental groups. When the confluence angle was 45°, a near overall increase in the depositional volume and a decrease in the depositional gradient was observed relative to experiments with a 90° confluence angle. A reduction in the confluence angle limits the tributary channel flow penetration into the main channel (Best, 1988), reducing the exposure of the tributary sediment to main channel entraining forces. In the context of experiments 1-15, with a greater confluence angle, the penetration of the tributary channel exhibited a greater extent. Increasing the confluence angle caused a greater mutual deflection of flows, further segregating the tributary and main channel flows (Best, 1988). This factor, coupled with the increased velocity, allowed the tributary sediment load to rapidly pass through the confluence zone when the confluence angle was greater rather than be deposited in the tributary channel.

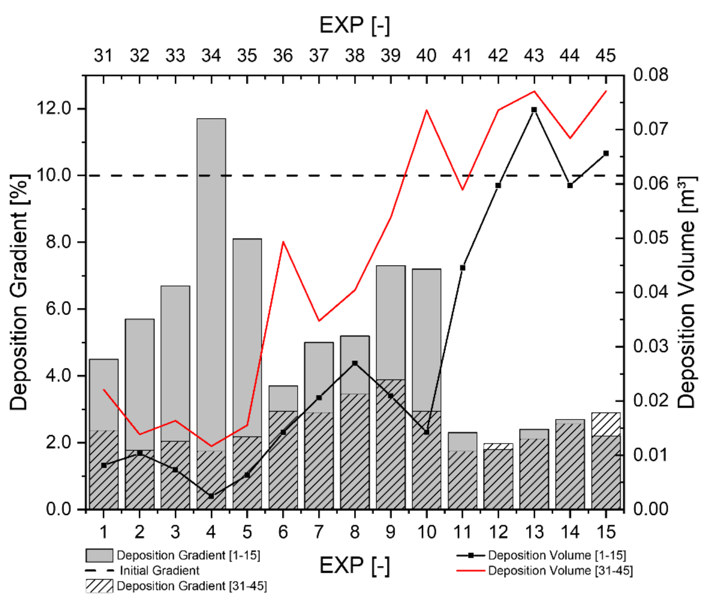

Figure 9 Gradients and volumes of deposited sediment in the tributary channel for experiments 1-15 and 31-45.

https://doi.org/10.5194/egusphere-2023-2432
Preprint. Discussion started: 13 December 2023

3.4 Statistical evidence of factors impacting confluence morphology

3.4.1 Overview

Only factors that had a significant effect (Table 4) on the response variables are discussed. The focus of the statistical analysis is to determine the dominant controls over confluence morphology. For this reason, tributary channel depositional behavior is not included as a response variable.

Table 4 Introduced factors and their impact on confluence morphology, green indicates the factor had a significant impact on one or more groups of the response variable. P-values from overall mean comparison tests are included.

Factor	z_{max}	z_{min}	Deposition area	Deposition volume	Erosion area	Erosion volume	Bar area	Bar length	Bar width	Scour area	Scour length	Scour width
Sediment concentration	.001	.30	.09	.00101	.19	.015	2.85E-4	.059	< 0.001	4.38E-4	3.63E-4	.30
Discharge	.004	<.0001	.047	<.0001	.007	<.0001	1.89E-4	<.0001	.14	< .0001	< .0001	<.0001
Tributary gradient	.20	.78	.82	.24	.96	.50	.27	.79	.21	.33	.35	.55
Confluence angle	.46	0.022	.91	.40	0.84	.67	.25	.81	.37	.23	.047	.267

3.4.2 Sediment concentration

Table 5 and Fig. 10 show that sediment concentration had a significant impact on 7 out of 12 response variables. Increased sediment concentration provoked depositional patterns, while decreased sediment concentration enhanced erosional patterns. Post hoc testing further revealed patterns caused by the sediment concentration (Table 5). Unsurprisingly the majority of the significant differences in mean response values occurred between 5 % and 10 % sediment concentration groups. The maximum deposition depth was significantly reactive to all sediment concentrations, as the sediment concentration increased the deposition depth increased, but is regulated by the local flow depth. When the sediment concertation was 7.5 %, the response variables did not significantly differ from those of the 5 % and 10 % groups.

https://doi.org/10.5194/egusphere-2023-2432
Preprint. Discussion started: 13 December 2023

Table 5 Sediment concentration and its impact on the response variables, (σ) is the standard deviation. Post hoc testing is summarized with letters A, B, and C. If sediment concentration groups share a letter then there is no significant difference in the pairwise comparisons of means; if the letters are different then a significant difference was detected. For example, the mean Z_{max} for each sediment concentration group was significantly different (A, B, C), but the mean deposition volume for sediment 7.5 % and 10 % concentration groups did not significantly differ from each other (B, B) but were significantly different from the mean deposition volume when the sediment concentration was 5 % (A).

	σ								
Response Variable	**5%**	**7.5%**	**10%**	**Test**	**Difference in Means**	**Post hoc Test**	**5**	**7.5**	**10**
[-]	**[-]**	**[-]**	**[-]**	**[-]**	**[-]**	**[-]**	**[%]**	**[%]**	**[%]**
Z_{max} [m]	0.01	0.02	0.02	ANOVA (F = 18.5)	Yes	Tukey-Test	A	B	C
Z_{min} [m]	0.02	0.02	0.02	ANOVA (F = 1.2)	No				
Deposition area [m²]	1.00	0.68	0.85	ANOVA (F = 2.4)	No				
Deposition volume [m³]	0.02	0.05	0.06	ANOVA (F = 8.2)	Yes	Tukey-Test	A	B	B
Erosion area [m²]	1.02	0.74	0.87	ANOVA (F = 1.7)	No				
Erosion volume [m³]	0.03	0.02	0.01	Welch ANOVA (F = 4.9)	Yes	Games-Howell	A	A/B	B
Deposition bar area [m²]	0.47	0.72	1.01	Welch ANOVA (F = 11.5)	Yes	Games-Howell	A	B	B
Length bar [m]	0.88	0.57	0.74	ANOVA (F = 3.0)	No				
Width bar [m]	0.07	0.08	0.09	ANOVA (F = 13.3)	Yes	Tukey-Test	A	B	B
Scour area [m²]	0.47	0.30	0.22	Welch ANOVA (F= 10.6)	Yes	Games-Howell	A	A	B
Length scour [m]	0.96	0.96	0.67	ANOVA (F = 9.7)	Yes	Tukey-Test	A	B	B
Width scour [m]	0.14	0.12	0.14	ANOVA (F = 1.3)	No				

Adjustments in deposition and erosion areas allowed for the majority of the incoming sediment load to pass through the confluence. However, given the differences in sediment loads, rapid mutual adjustments were morphologically represented by the same general patterns but with less erosion and more aggradation as sediment concentration increases. The differences in mean response values between the experiments with 5 % and 10 % tributary sediment concentrations and the similarities to the mean response values, when the sediment concentration was 7.5 %, can be attributed to this process.

https://doi.org/10.5194/egusphere-2023-2432
Preprint. Discussion started: 13 December 2023

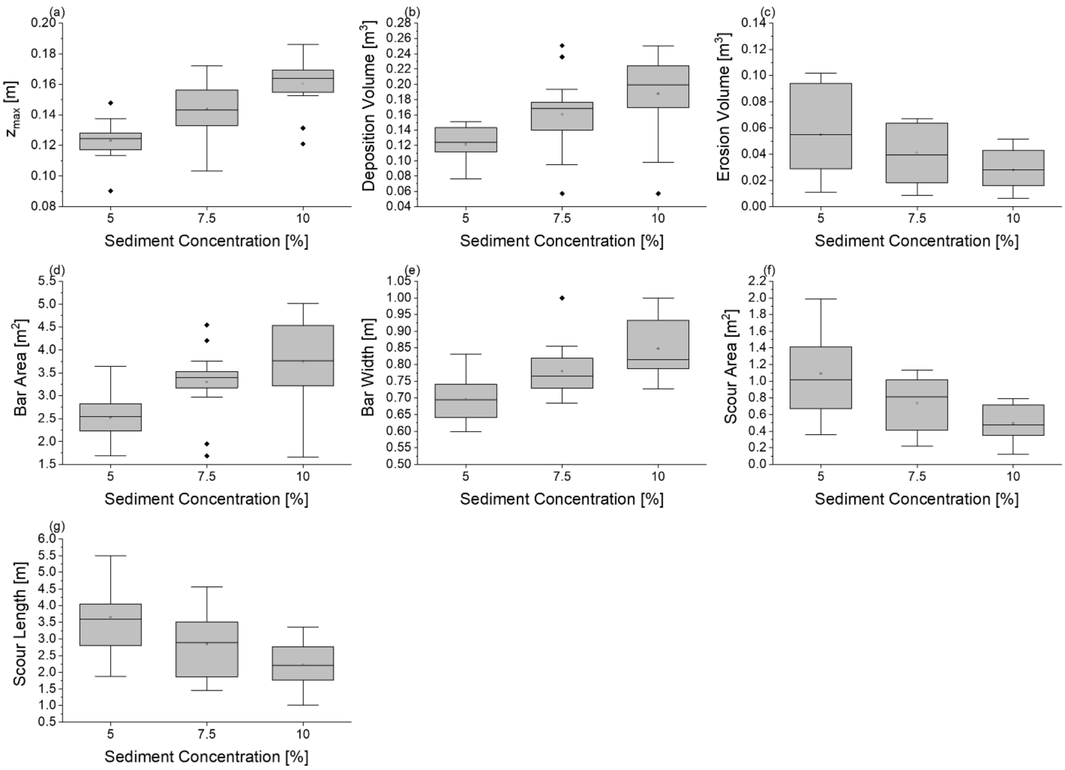

Figure 10 Boxplots from ANOVA and Welch ANOVA results for all response variables that showed a significant difference in mean values with sediment concentration as the factor.

3.4.3 Combined discharge

Table 6 and Fig. 11 show that the discharge significantly affected 11 out of 12 response variables. Generally, erosional processes increased with increasing discharge as the transport capacity of the main channel flow increased. At lower discharges with limited transport capacity, erosional processes were comparatively reduced. However, certain instances revealed increased depositional properties with increasing discharge (Fig. 11a and 11d). This most apparently occurred between the 16.5 l s^{-1} and 49.5 l s^{-1} combined discharge experiments. A deposition cone formed across all sediment concentrations when the combined discharge was 16.5 l s^{-1}. Unlike the bar or transitional morphology, the deposition cone does not occupy the separation zone and is characterized by a short longitudinal extent while protruding furthest into the main channel from

https://doi.org/10.5194/egusphere-2023-2432
Preprint. Discussion started: 13 December 2023

the tributary channel. At discharges at and above 49.5 l s^{-1}, the depositional patterns shifted, and sediment was entrained and deposited in the separation zone. The separation zone is the largest sink for tributary transported sediment; the occupying bar can only be as big as the hydraulic zone, which is the same size for a given discharge ratio (Best, 1987; 1988). This explains the subtle differences in depositional properties once the combined discharge exceeded 49.5 l s^{-1}.

Table 6 Discharge and its impact on the response variables (σ) is the standard deviation. Post hoc testing is summarized with letters A, B, C, and D if discharge groups share a letter then there is not a significant difference in the pairwise comparisons of means, if the letters are different then a significant difference was detected.

	σ												
Response Variable	**16.5**	**49.5**	**82.5**	**115.5**	**148.5**	**Test**	**Diff. in means**	**Post Hoc Test**	**16.5**	**49.5**	**82.5**	**116**	**149**
[-]	**[l s^{-1}]**	**[l s^{-1}]**	**[l s^{-1}]**	**[l s^{-1}]**	**[l s^{-1}]**	**[-]**	**[-]**	**[-]**	**[l s^{-1}]**	**[l s^{-1}]**	**[l s^{-1}]**	**[l s^{-1}]**	**[l s^{-1}]**
Z_{max} [m]	0.02	0.02	0.02	0.02	0.02	ANOVA (F = 4.5)	YES	Tukey-Test	A	A/B	A/B	A/B	B
Z_{min} [m]	0.01	0.01	0.02	0.01	0.02	ANOVA (F = 10.7)	YES	Tukey-Test	A	B	B	B	B
Deposition [m^2]	1.07	0.52	0.93	0.77	0.68	ANOVA (F = 2.7)	YES	Tukey-Test	A	A	A	A	A
Deposition [m^3]	0.02	0.03	0.04	0.04	0.05	ANOVA (F = 9.3)	YES	Tukey Test	A	B	B	B	B
Erosion area [m^2]	1.08	0.52	0.92	0.66	0.63	ANOVA (F = 4.1)	YES	Tukey Test	A	A	A/B	B	A/B
Erosion volume [m^3]	0.004	0.01	0.02	0.02	0.02	Welch ANOVA (F = 28.9)	YES	Games-Howell	A	B	B/C	C	C
Bar area [m^2]	0.52	0.91	0.79	0.71	0.54	ANOVA (F= 7.2)	YES	Tukey Test	A	B	B	B	B
Length bar [m]	0.62	0.33	0.38	0.5	0.34	ANOVA (F = 22.0)	YES	Tukey Test	A	B	B	B	B
Width bar [m]	0.06	0.11	0.11	0.12	0.06	ANOVA (F = 1.9)	NO						
Scour area [m^2]	0.17	0.24	0.33	0.42	0.38	ANOVA (F = 9.1)	YES	Tukey Test	A	A/B	B/C	C	C
Length scour [m]	0.8	0.63	0.76	0.92	0.87	ANOVA F = 8.4)	YES	Tukey Test	A	A	A/B	B	B
Width scour [m]	0.05	0.08	0.06	0.06	0.06	ANOVA (F = 36.9)	YES	Tukey Test	A	B	C	D	D

Pair-wise post hoc comparisons of maximum deposition depth indicated a significant difference in mean values between the lowest and highest combined discharge experiments while revealing similarities among intermediate discharge scenarios. These similarities could be attributed to the combined flows regulating the depositional depth, which does not exceed the flow depth. The observed differences can be attributed to the increased sediment load and associated morphological changes with increasing discharge.

https://doi.org/10.5194/egusphere-2023-2432
Preprint. Discussion started: 13 December 2023

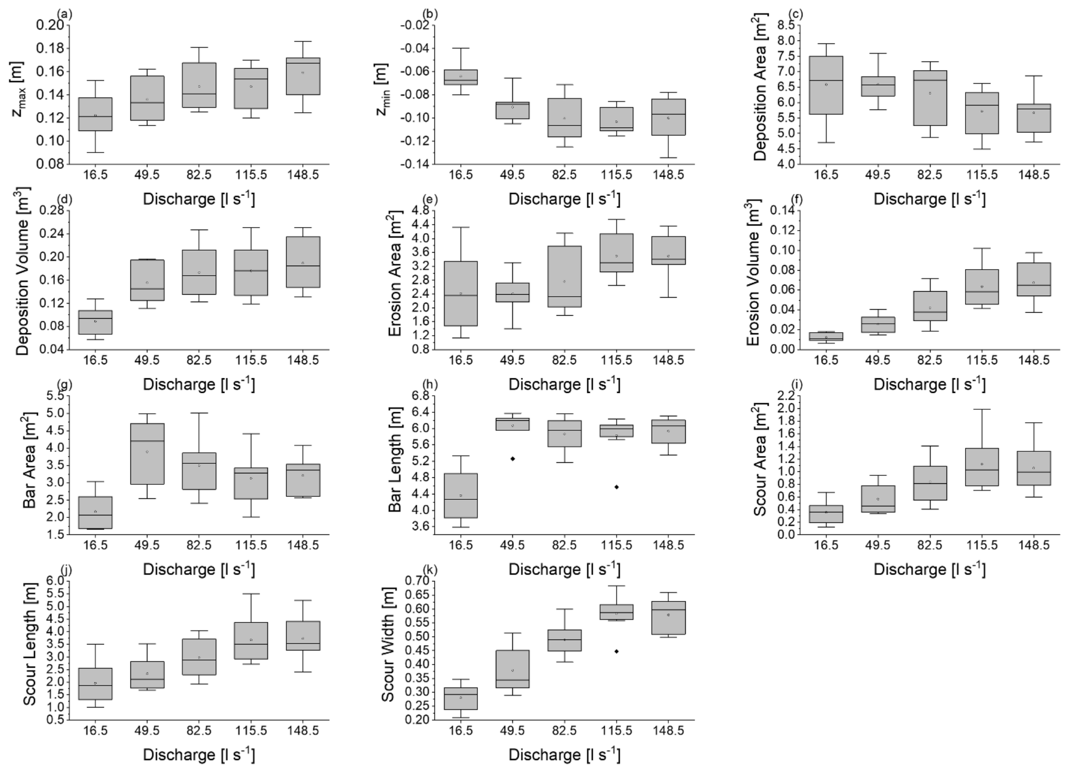

Figure 11 Boxplots from ANOVA and Welch ANOVA results for all response variables that showed a significant difference in mean values with combined discharge as the factor.

3.4.4 Confluence angle

Surprisingly, the confluence angle only had a significant influence on 2 out of 12 of the response variables (Table 7). The confluence angle did have a decisive impact on scour depth (Fig. 12a). This could be attributed to the degree of turbulence increasing with increasing confluence angle which enhanced the ability of the flow to scour the bed (Mosley, 1976). Reducing the confluence angle allowed for improved mixing which in turn decreased the turbulence in the confluence producing shallower scour.

https://doi.org/10.5194/egusphere-2023-2432
Preprint. Discussion started: 13 December 2023

Table 7 Confluence angle and its impact on the response variables. Post hoc testing was not required since there are only 2 groups to compare, σ is the standard deviation.

Response Variable	σ		Test	Difference in means
	45°	90°		
[-]	[-]	[-]	[-]	[-]
Z_{max} [m]	0.02	0.02	T-Test (t statistic = - 0.742)	NO
Z_{min} [m]	0.02	0.02	T Test (t statistic = -2.37)	YES
Deposition Area [m²]	0.96	0.85	T Test (t statistic = 0.109)	NO
Deposition Volume [m³]	0.06	0.05	T Test (t statistic = -0.843)	NO
Erosion Area [m²]	0.98	0.87	T Test (t statistic = -0.199)	NO
Erosion Volume [m³]	0.03	0.03	T Test (t statistic = -0.425)	NO
Deposition Bar Area [m²]	0.75	0.95	T Test (t statistic = 1.169)	NO
Length Bar [m]	0.81	0.77	T Test (t statistic = 0.238)	NO
Width Bar [m]	0.10	0.10	T Test (t statistic = 0.916)	NO
Scour Area [m²]	0.52	0.36	T Test (t statistic = -1.212)	NO
Length Scour [m]	1.22	0.88	T Test (t statistic = -2.04)	YES
Width Scour [m]	0.12	0.14	T Test (t statistic = 1.125)	NO

Additionally, the confluence angle had an impact on the length of the scour (Fig. 12b). Enhanced mixing of confluent flows, and a reduced hydraulic separation zone created conditions where the scour generally occupied a greater area but produced a shallower scour depth. However, the width of the bar was relatively unchanged (Fig. 9c) in response to the confluence angle; the increased scour area was represented by an increase in scour length. While the penetration of the tributary channel was reduced, the transport capacity of the main channel was still sufficient to mobilize a similar volume of sediment (Fig. 9f).

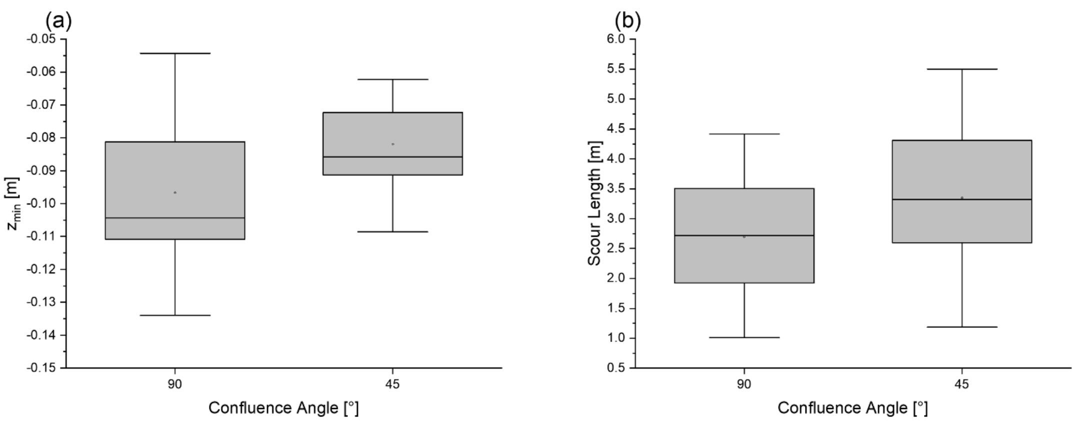

Figure 12 Boxplots from T-Test results for all response variables that showed a significant difference in mean values with the confluence angle as the factor

https://doi.org/10.5194/egusphere-2023-2432
Preprint. Discussion started: 13 December 2023

4 Discussion

The confluence angle has been established as one of the main drivers of confluence morphology and the spatial distribution of the hydraulic zones for lowland confluences. However, for mountain river confluences during events with intense bedload transport it had a minimal effect, corroborating hypothesis 1. The scour area and depth were the only response variables sensitive to the confluence angle. Decreasing the confluence angle limited the extent of the separation zone (compare Mosley, 1976; Best, 1987). The zone of maximum velocity responded sympathetically to the size of the flow separation zone (compare Best, 1987). When more channel was available for the zone of maximum velocity, the velocity decreased, causing shallower scour, which is consistent with the findings of Mosley (1976) and Best (1988). In contrast, increasing the confluence angle increased the local velocity and transport capacity and caused greater penetration of the tributary flow. These combined aspects provide evidence that the transport capacity of the main channel is enhanced at higher confluence angles, which was reflected in the tributary depositional volumes and gradients. The tributary channel gradient responding to the transport capacity in mountain rivers has been previously observed (Mueller & Pitlick, 2005; Trevisani et al., 2010). Mueller and Pitlick (2005) suggest that forced changes in gradient are offset by adjustments to width, depth, and bed surface texture to maintain a balance between the intensity and frequency of bed load transport. In confined channels, width adjustments are not possible, resulting in extensive deposition in the channel. The main differences in sediment depositional patterns and mechanisms from adjusting the tributary channel gradient were observed in the tributary channel, while the main channel was largely unchanged. This indicates that with a sustained and abundant sediment supply and relatively uniform main channel hydraulic conditions, the morphologic development of the confluence is not significantly impacted by changes in the tributary channel gradient.

Referring to hypothesis 2, the same geomorphic units and morphological patterns occurred for all experimental groups and channel configurations, which establishes the dominance of channel discharges over the confluence. Adjustments to sediment concentration were shown by a range of deposition and erosion depths, volumes, and varying extents of the geomorphic units. Interaction between discharge and sediment shows clear trends of coarsening or fining at specific sites (Fig. 13, Appendix 10) for all the

https://doi.org/10.5194/egusphere-2023-2432
Preprint. Discussion started: 13 December 2023

introduced factors. However, trends relating sediment concentration or channel geometry to coarsening or fining are not apparent since the same general morphological patterns consistently occurred, which in turn caused similar hydraulic conditions to develop. Grain size distribution curves from the tributary channel near the confluence, the deposition cone or bar, and the recovery zone further illustrate the selective bedload transport occurring in the confluence zone. Consistent across all experiments, the deposited material in the tributary was finer than the input mix (Fig. 13a to 13c, Appendix 10). For experiments with the 10 % tributary gradient, this can be explained by the regressive aggradation occurring in the tributary channel, which reduced the gradient of the tributary and, thus, the transport capacity. For experiments with a 5 % tributary gradient, the transport capacity of the tributary was saturated, which caused intense progressive deposition of all grain sizes in the channel despite the increased depositional gradient. Samples taken from the scour hole (Fig. 13d to 13f, Appendix 10) showed an overall coarsening, illustrating the enhanced transport capacity through this zone. The separation zone bar was formed in a region of low flow velocity relative to the main channel, which is reflected in the associated grain size distributions (Fig. 13h and 13i, Appendix 10). The samples taken from the lowest discharge experiments were from the deposition cone; the cone did not occupy the hydraulic separation zone and was exposed to the main channel flow. Accordingly, the samples showed a general coarsening pattern of the finer grain fractions and a fining of the larger grain size fractions (Fig. 13g, Appendix 10). The zone of flow recovery is characterized by decreased turbulence and more uniform flow patterns and bed morphology (compare Best, 1987; 1988). As a result, no hydraulic or morphologic structures existed that influenced the velocity distribution throughout this portion of the channel. This is apparent in Fig. 13j to 13l where the samples taken across all experiments showed the least deviation from the plotted line of the input material. A slight but overall coarsening is apparent, caused by the increased velocity from the combined channel flow and the resulting selective bedload transport.

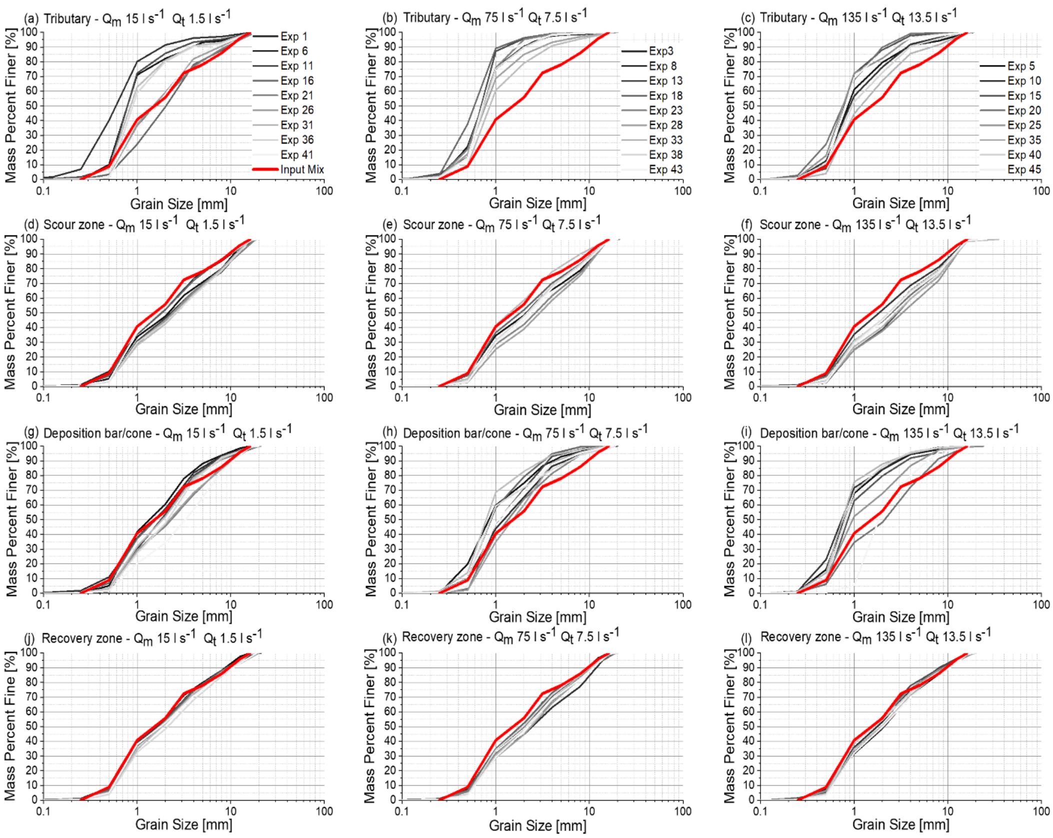

Figure 13 Grain size distribution curves from samples taken from the tributary channel (a-c), the scour hole (d-f), the deposition cone or bar (g-i), and the recovery zone (j-l) for the lowest, middle, and highest experimental discharges, Q_m and Q_t denote main and tributary channel discharges, respectively.

5 Conclusion

The channel discharges and then the tributary sediment concentration are the most impactful factors influencing mountain river confluence morphology during events with intense bedload transport. This conclusion contrasts with the findings of the a body of literature dealing with the controls of river confluences. Mountain river confluences are influenced by characteristics unique to mountain regions, including the availability of massive amounts of sediment and frequent localized flooding. Because of these combined

https://doi.org/10.5194/egusphere-2023-2432
Preprint. Discussion started: 13 December 2023

factors, adjustments to channel geometry did not significantly impact the morphological development of the confluence. However, adjustments did cause an apparent response to the depositional mechanisms in the tributary channel. A progressive or regressive aggradation of tributary sediment occurred, indicating which channel was limiting in terms of transport capacity. Rapid mutual adjustments occurred as the channel adjusted to the hydraulic and sediment inputs as the system tended towards an equilibrium state. Tending towards an equilibrium morphology was characterized by the geomorphic units, which were indicators of the flood magnitude. When sediment concentration was fixed, and the discharge was adjusted, the morphology responded to the combined channel flows downstream of the confluence. However, the morphological patterns are mainly unaffected when the discharge is fixed and the sediment concertation is adjusted. Therefore, the combined discharge determines the overall morphology and the development of specific geomorphic units, and the sediment concentration controls the morphological extent of the units. These aspects illustrate that the geomorphological spatial patterns at mountain river confluences are unique and require special attention for flood risk management. Further work should also include assessing ecologically valuable protection measures, including sediment buffer zones.

https://doi.org/10.5194/egusphere-2023-2432
Preprint. Discussion started: 13 December 2023

6 Appendix

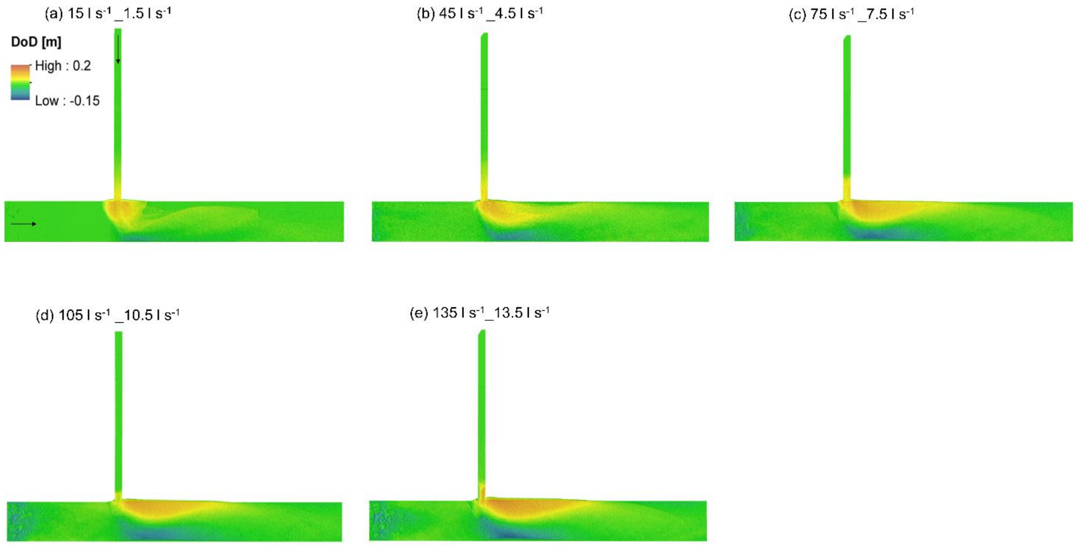

A 1 Confluence morphology for experiments 1-5 with 5 % sediment concentration, a 90° confluence angle, and a 10 % tributary gradient.

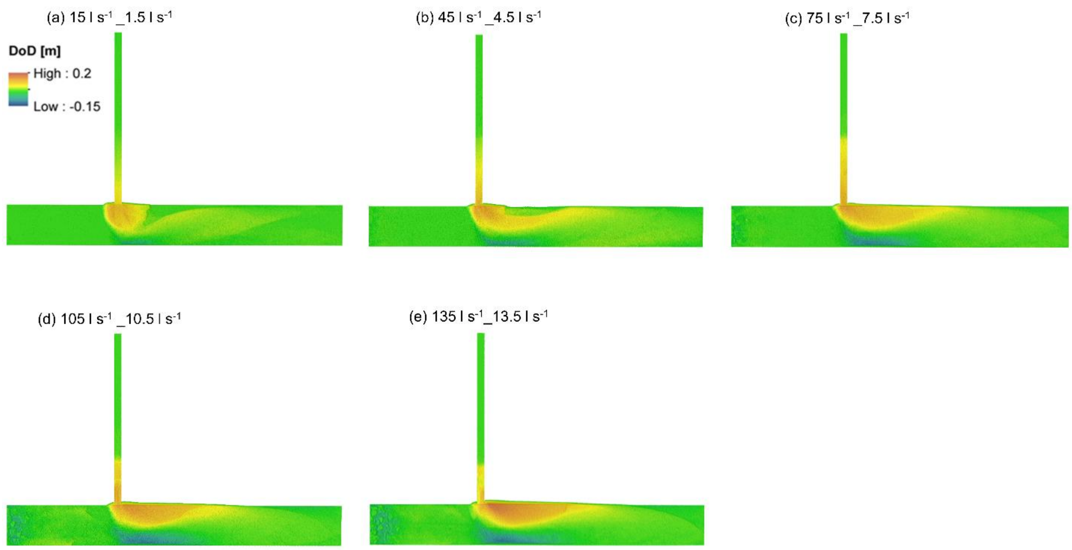

A 2 Confluence morphology for experiments 6-10 with 7.5 % sediment concentration, a 90° confluence angle, and a 10 % tributary gradient.

https://doi.org/10.5194/egusphere-2023-2432
Preprint. Discussion started: 13 December 2023

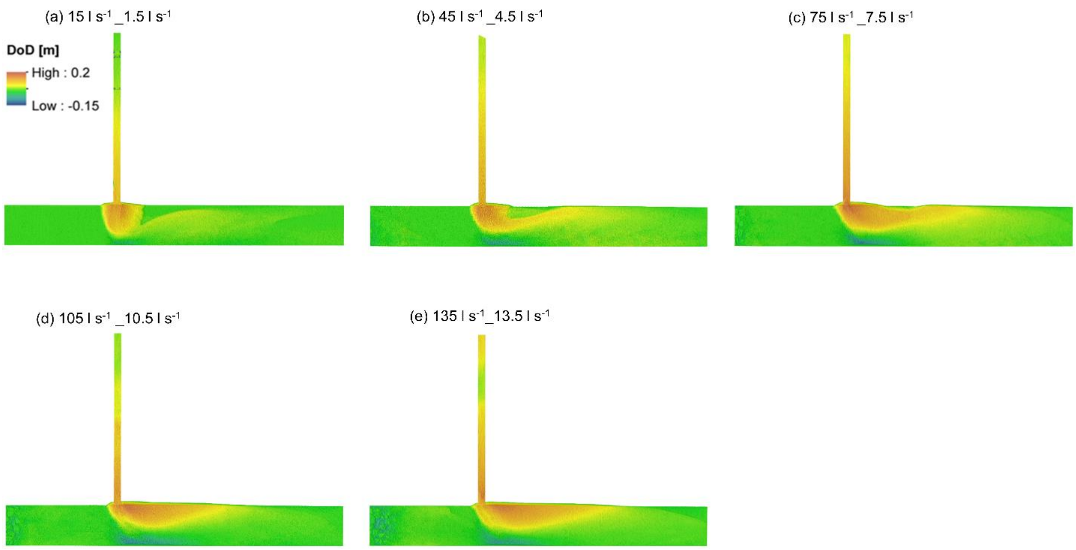

A 3 Confluence morphology for experiments 11-15 with 10 % sediment concentration, a 90° confluence angle, and a 10 % tributary gradient.

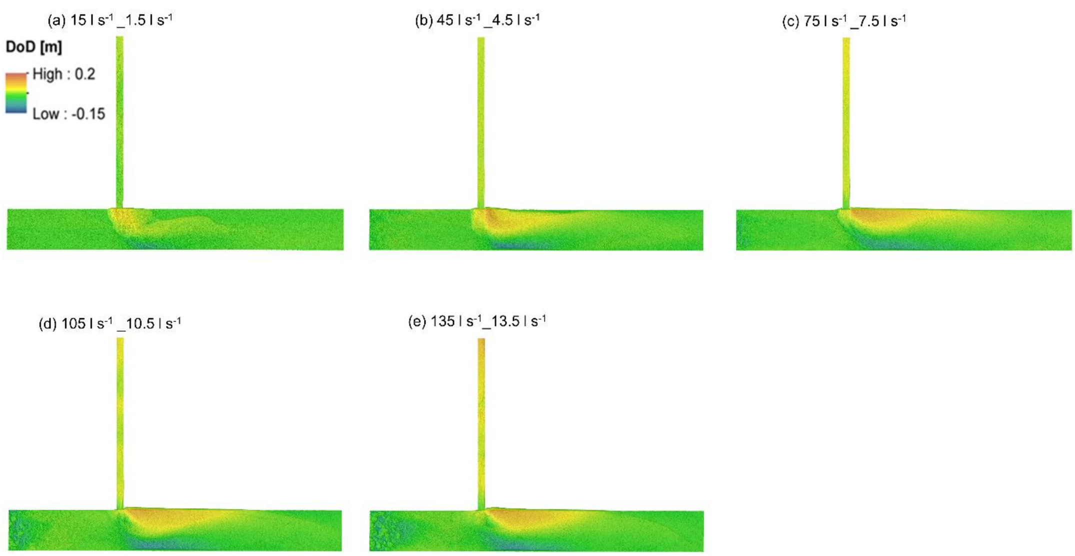

A 4 Confluence morphology for experiments 16-20 with 5 % sediment concentration, a 90° confluence angle, and a 5 % tributary gradient.

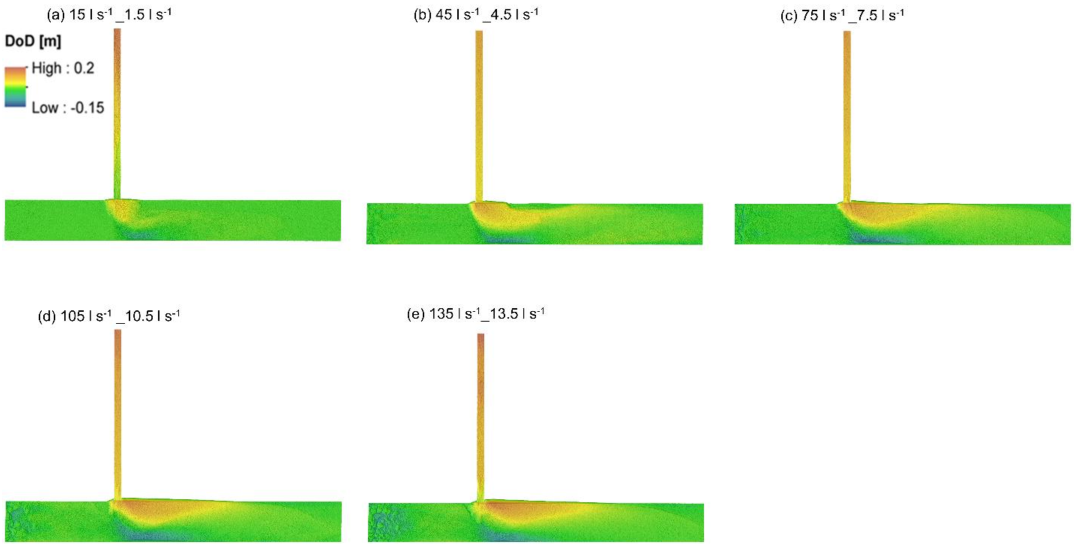

A 5 Confluence morphology for experiments 21-25 with 7.5 % sediment concentration, a 90° confluence angle, and a 5 % tributary gradient.

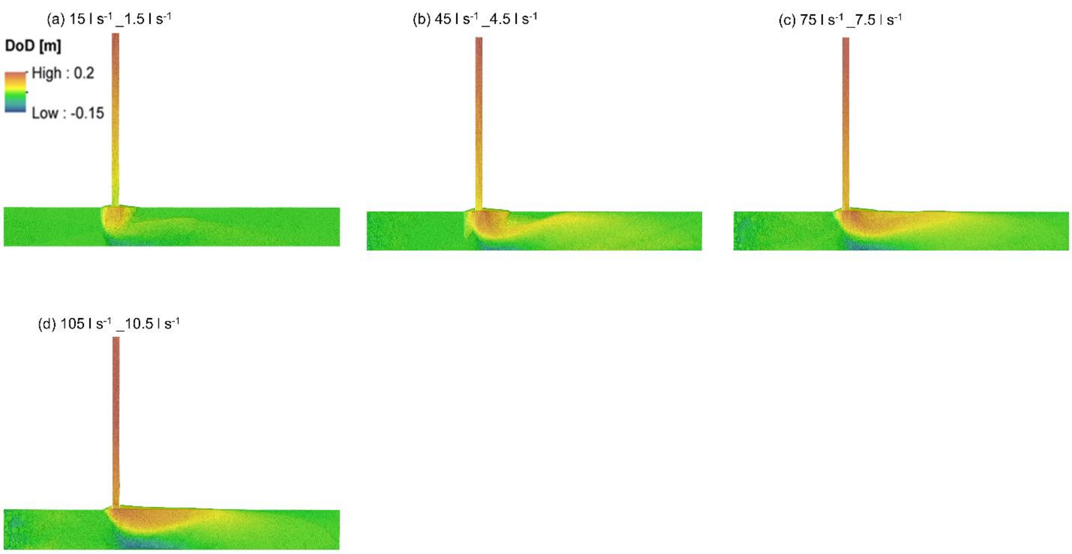

A 6 Confluence morphology for experiments 26-29 with 10 % sediment concentration, a 90° confluence angle, and a 5 % tributary gradient.

https://doi.org/10.5194/egusphere-2023-2432
Preprint. Discussion started: 13 December 2023

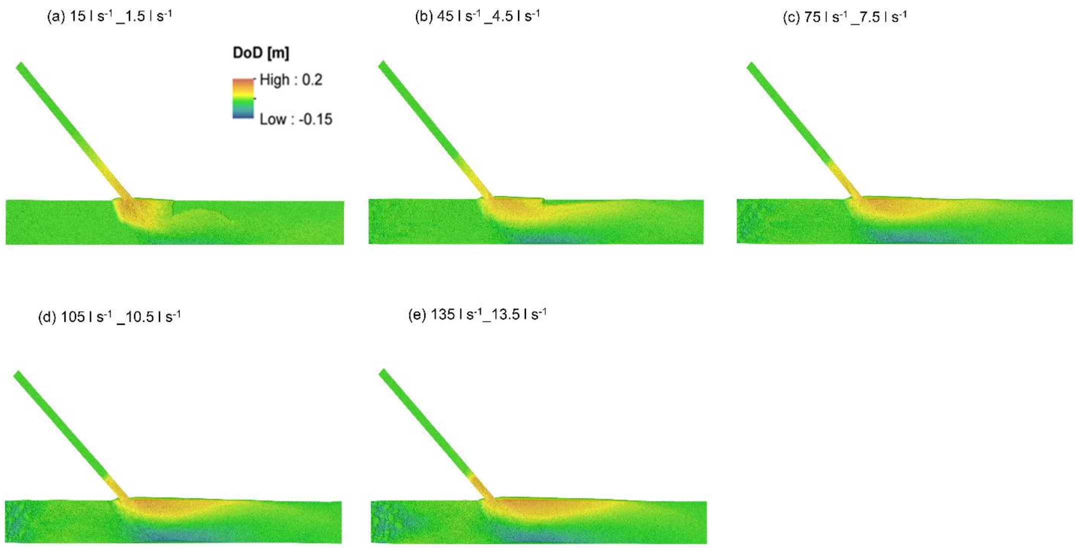

A 7 Confluence morphology for experiments 31-35 with 5 % sediment concentration, a 45° confluence angle, and a 10 % tributary gradient.

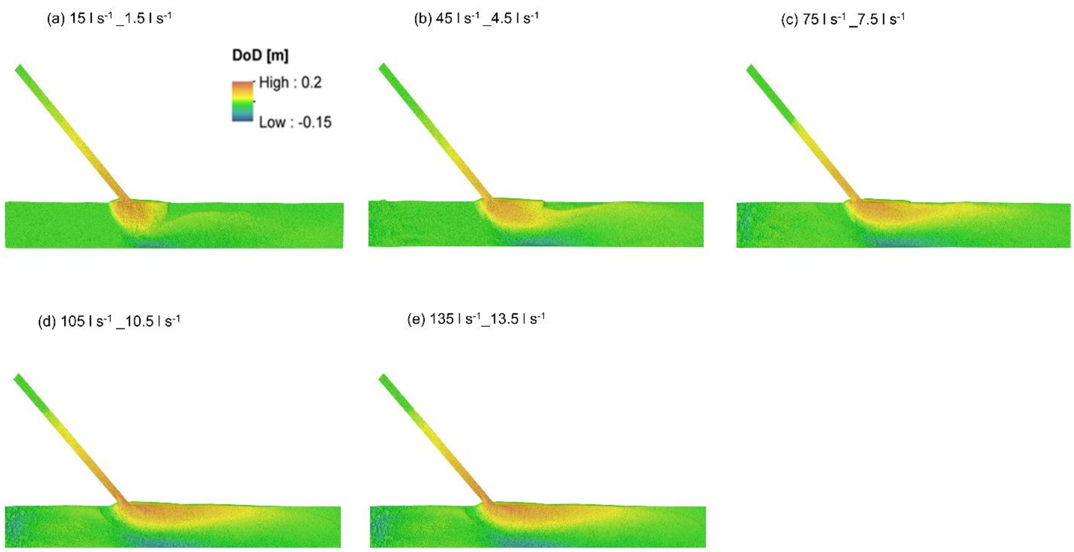

A 8 Confluence morphology for experiments 36-40 with 7.5 % sediment concentration, a 45° confluence angle, and a 10 % tributary gradient.

https://doi.org/10.5194/egusphere-2023-2432
Preprint. Discussion started: 13 December 2023

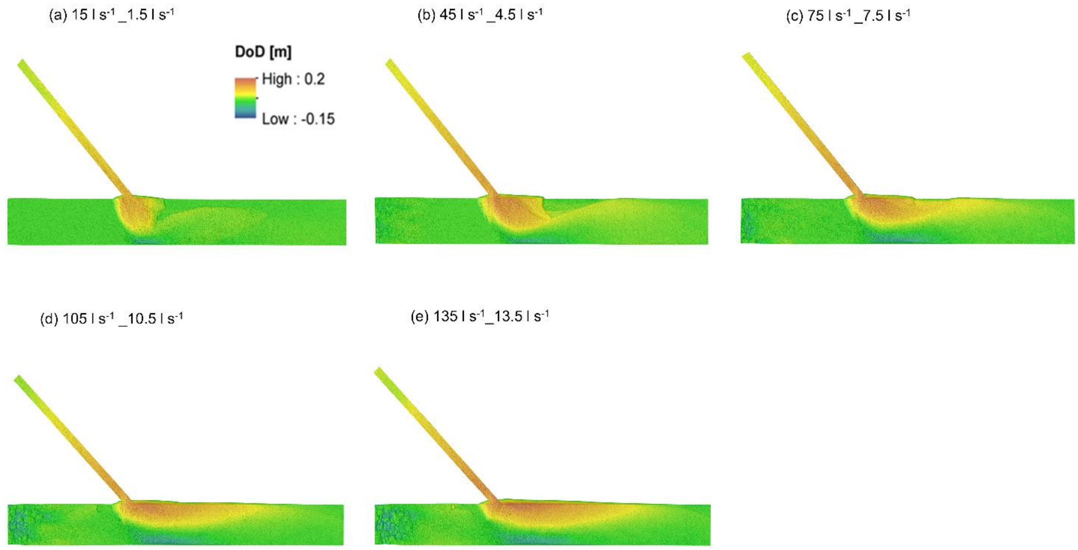

A 9 Confluence morphology for experiments 41-45 with 10 % sediment concentration, a 45° confluence angle, and a 10 % tributary gradient.

https://doi.org/10.5194/egusphere-2023-2432
Preprint. Discussion started: 13 December 2023

A 10 Characteristic grain size for all experiments from samples taken in the tributary channel, the geomorphic unit (cone, transitionary, bar, or scour hole) and the recovery zone. Green or red indicates the sampled grain size was smaller or larger then the input mix grain size, respectively.

Exp	D16				D50				D84				Dm			
	Trib.	Depo.	Scour	Recov.	Trib.	Depo.	Scour	Recov.	Trib.	Depo.	Scour	Recov.	Trib.	Depo.	Scour	Recov.
[-]	[mm]	[mm]	[mm]	[mm]	[mm]	[mm]	[mm]	[mm]	[mm]	[mm]	[mm]	[mm]	[mm]	[mm]	[mm]	[mm]
Input	0.7	0.7	0.7	0.7	1.4	1.4	1.4	1.4	6.2	6.2	6.2	6.2	2.8	2.8	2.8	2.8
1	0.5	0.6	0.7	0.6	0.8	1.4	2.2	1.7	2.4	4.3	9.2	6.2	1.8	2.5	4.0	3.0
2	0.5	0.6	0.7	0.6	0.9	1.7	2.1	1.5	2.5	5.6	9.4	6.5	1.5	2.9	4.1	3.1
3	0.4	0.5	0.7	0.5	0.8	0.9	2.2	1.4	1.6	2.9	9.6	6.0	1.1	1.8	4.1	2.9
4	0.5	0.5	0.6	0.6	0.9	0.9	1.7	1.4	3.7	2.9	8.6	6.5	2.6	1.9	3.8	3.3
5	0.6	0.5	0.7	0.6	0.9	0.8	2.5	1.3	2.8	2.0	10.0	6.2	2.0	1.5	4.4	3.2
6	0.3	0.6	0.6	0.6	0.6	1.6	1.9	1.7	1.3	4.7	7.6	6.2	1.2	2.8	3.6	3.4
7	0.4	0.6	0.8	0.6	0.7	1.0	3.4	1.6	0.9	3.2	12.3	6.5	0.8	2.0	5.7	3.2
8	0.4	0.6	0.6	0.5	0.8	1.3	2.0	1.2	1.6	3.8	9.1	6.0	1.1	2.4	4.0	3.1
9	0.6	0.6	0.7	0.6	0.9	0.9	2.3	1.4	1.9	3.7	7.3	6.7	1.4	2.5	3.8	3.5
10	0.5	0.4	0.7	0.7	0.9	0.8	1.9	1.8	3.0	2.0	9.3	6.4	1.9	1.3	4.0	2.4
11	0.6	0.8	0.7	0.7	0.8	1.8	2.4	2.3	1.9	5.3	10.3	9.1	1.7	3.0	4.5	4.2
12	0.5	0.7	0.7	0.7	0.8	1.6	2.8	3.0	2.6	3.9	11.2	11.2	1.6	2.6	5.0	3.2
13	0.5	0.6	0.9	0.7	0.7	1.1	5.8	1.5	1.0	3.2	13.1	7.2	0.9	1.9	6.8	3.4
14	0.4	0.6	0.8	0.6	0.8	1.3	5.4	1.3	1.9	3.4	13.0	4.4	1.3	2.1	6.6	2.7
15	0.6	0.6	0.8	0.7	0.8	0.9	3.1	1.6	1.8	2.7	11.0	6.1	1.2	1.8	5.0	3.8
16	0.8	0.6	0.7	0.6	2.0	1.7	1.9	1.7	6.4	5.6	3.4	6.4	3.5	3.2	3.8	3.2
17	0.4	0.7	0.9	0.7	0.7	1.7	4.1	1.8	0.9	5.2	3.8	6.8	0.7	2.9	5.9	3.6
18	0.3	0.6	0.6	0.6	0.6	0.9	1.9	1.6	1.0	2.6	3.7	6.0	0.8	1.5	3.8	3.1
19	0.4	0.6	0.8	0.7	0.7	1.4	3.3	1.8	1.0	5.3	3.8	7.0	0.9	2.8	5.1	3.5
20	0.4	0.7	0.7	0.6	0.8	2.2	2.6	1.4	1.7	6.4	3.9	6.4	1.1	3.4	4.6	3.1
21	0.7	0.7	0.7	0.7	1.7	2.4	2.5	2.0	6.4	7.6	3.6	7.9	3.2	3.9	4.4	3.7
22	0.5	0.8	0.8	0.7	0.7	1.9	3.3	1.7	1.0	4.9	4.1	6.6	0.9	3.0	5.8	3.3
23	0.4	0.7	0.7	0.6	0.8	1.4	2.8	1.6	1.4	4.8	3.8	7.1	1.0	2.7	4.7	3.4
24	0.5	0.6	0.7	0.6	0.8	1.3	2.4	1.6	1.6	4.3	3.7	6.0	1.1	2.6	4.3	3.3
25	0.5	0.6	0.8	0.6	0.8	1.0	3.4	1.7	2.2	3.7	3.8	6.8	1.4	2.1	5.3	3.4
26	0.7	0.8	0.7	0.7	1.6	2.3	2.6	2.0	5.0	7.8	3.8	7.7	2.9	4.0	4.8	3.8
27	0.5	0.9	0.8	0.7	0.8	2.3	3.1	1.7	1.0	5.6	3.8	6.8	0.9	3.3	5.1	3.4
28	0.5	0.7	0.8	0.7	0.8	1.6	3.1	1.7	1.9	3.7	3.9	7.8	1.5	2.4	5.4	3.7
29	0.5	0.7	0.7	0.7	0.8	1.7	2.6	1.8	1.8	5.9	3.8	6.6	1.3	3.2	4.6	3.4
30	-	-	-	-	-	-	-	-	-	-	-	-	-	-	-	-
31	0.6	0.7	0.8	0.7	0.9	1.9	2.8	1.9	2.6	5.7	10.0	6.9	2.0	3.2	4.6	3.6
32	0.5	0.5	0.7	0.7	0.8	0.9	2.0	1.9	1.7	3.5	7.1	7.5	1.2	2.1	3.7	3.7
33	0.6	0.52	0.7	0.7	0.9	0.8	1.5	1.7	2.8	2.2	6.0	7.6	1.9	1.5	3.1	3.6
34	0.6	0.6	0.7	0.7	0.9	0.9	1.9	1.8	2.9	3.5	6.4	7.3	1.8	2.1	3.3	3.5
35	0.6	0.5	0.8	0.7	1.2	0.8	3.0	1.7	3.8	1.7	11.0	6.6	2.6	1.3	5.1	3.4
36	0.6	0.8	0.7	0.7	0.9	2.2	2.7	1.8	2.8	5.9	10.1	7.1	2.1	3.3	4.6	3.7
37	0.5	0.7	0.7	0.7	0.8	1.5	1.6	1.7	1.7	5.9	9.0	7.2	1.2	3.1	3.8	3.7
38	0.5	0.6	0.7	0.6	0.8	0.9	2.2	1.5	1.6	4.0	8.6	5.8	1.1	2.4	4.0	3.1
39	0.6	0.55	0.7	0.6	0.8	0.9	2.5	1.4	1.9	3.4	9.8	5.7	1.3	2.1	4.4	3.0
40	0.6	0.5	0.7	0.7	1.0	0.8	2.5	1.9	3.3	1.9	10.0	5.9	2.0	1.3	4.4	3.3
41	0.7	0.9	0.7	0.7	1.7	3.4	1.8	1.9	4.0	8.5	7.3	7.8	2.9	4.7	3.5	3.8
42	0.5	0.9	0.7	0.7	0.8	2.3	2.5	1.9	1.0	4.8	10.4	6.3	0.9	3.1	4.6	3.3
43	0.5	0.6	0.7	0.7	0.8	1.1	2.4	1.8	1.1	3.6	9.4	7.8	1.0	2.2	4.3	3.8
44	0.6	0.6	0.7	0.7	0.9	1.0	2.3	2.0	1.8	3.0	9.7	7.7	1.3	1.9	4.3	3.7
45	0.6	1.2	0.8	0.8	0.8	1.9	2.5	2.5	1.8	5.0	10.4	7.4	1.4	3.02	4.6	3.9

https://doi.org/10.5194/egusphere-2023-2432
Preprint. Discussion started: 13 December 2023

7 Data Availability

Data are available from the corresponding author upon reasonable request.

8 Author Contributions

TSPO: Conceptualization, data curation, formal analysis, investigation, methodology, visualization, writing – original draft preparation (with input from all co-authors). TK: Formal analysis, data curation. BM: Conceptualization, methodology, writing – review and editing. JH: Formal analysis, investigation, writing – review and editing. AA: Conceptualization, writing – review and editing . FC: Conceptualization, supervision, project administration, funding acquisition, writing – review and editing BG: Conceptualization, supervision, project administration, funding acquisition, writing – review and editing.

9 Competing Interests

The authors declare that they have no conflict of interest.

10 Acknowledgements

The authors would like to thank the Autonomous Province of Bolzano - South Tyrol – Department of Innovation, Research, University and Museums for funding the project: Towards an Efficient Design of River Confluences to Manage Intense Sediment Impacts from Tributary Torrents (ECOSED_TT, contract number 24/34). This project and the accompanying funding provided the framework to conduct detailed investigations into mountain-river confluence hydraulics and morphology. Additionally, we acknowledge the funding of the Project Anid/Conicyt Fondecyt Regular Folio 1200091 titled “Unravelling the Dynamics and Impacts of Sediment-Laden Flows in Urban Areas in Southern Chile as a Basis for Innovative Adaptation (sedimpact)” led by the PI Bruno Mazzorana.

https://doi.org/10.5194/egusphere-2023-2432
Preprint. Discussion started: 13 December 2023

11 References

Aulitzky, H. (1980). Preliminary two-fold classification of debris torrents. Proceedings of "Interpraevent" Conference, Bad Ischl, Austria, Vol. 4, 285-309 (translated from German by G. Eisbacher). Internationale Forschungsgesellschaft, Interpraevent, Klagenfurt.

Aulitzky, H. (1989). The debris flows of Austria. Bulletin of the International Association of Engineering Geology, 40, 5-13. doi: 10.1007/BF0259033.

Baranovskiy, N. V. (2019). The development of application to software origin pro for informational analysis and forecast of forest fire danger caused by thunderstorm activity. Journal of Automation and Information Sciences, 51(4), 12-23. doi: 10.1615/jautomatinfscien.v51.i4.20.

Benda, L., Andras, K., Miller, D., & Bigelow, P. (2004). Confluence effects in rivers: Interactions of basin scale, network geometry, and disturbance regimes. Water Resources Research, 40(5), 1-15. doi: 10.1029/2003wr002583.

Best, J. L. (1987). Flow Dynamics at River Channel Confluences: Implications for Sediment Transport and Bed Morphology. Recent Developments in Fluvial Sedimentology, 27-35. doi: 10.2110/pec.87.39.0027.

Best, J. L. (1988). Sediment transport and bed morphology at river channel confluences. Sedimentology, 35, 481-498. doi: 10.1111/j.1365-3091.1988.tb00999.x.

Biron, P., Roy, A. G., Best, J. L., & Boyer, C. J. (1993). Bed morphology and sedimentology at the confluence of unequal depth channels. Geomorphology, 8(2-3), 115-129. doi: 10.1016/0169-555x(93)90032-w.

Blöschl, G., Hall, J., Parajka, J., Perdigão, R. A., Merz, B., Arheimer, B., Aronica, G. T., Bilibashi, A., Bonacci, O., Borga, M., Čanjevac, I., Castellarin, A., Chirico, G. B., Claps, P., Fiala, K., Frolova, N., Gorbachova, L., Gül, A., Hannaford, J., … Živković, N. (2017). Changing climate shifts timing of European floods. *Science*, *357*(6351), 588–590. doi: 10.1126/science.aan2506

https://doi.org/10.5194/egusphere-2023-2432
Preprint. Discussion started: 13 December 2023

Blöschl, G., Kiss, A., Viglione, A., Barriendos, M., Böhm, O., Brázdil, R., Coeur, D., Demarée, G., Llasat, M. C., Macdonald, N., Retsö, D., Roald, L., Schmocker-Fackel, P., Amorim, I., Bělínová, M., Benito, G., Bertolin, C., Camuffo, D., Cornel, D., … Wetter, O. (2020). Current European flood-rich period exceptional compared with past 500 years. *Nature*, *583*(7817), 560–566. Doi; 10.1038/s41586-020-2478-3

Boyer, C., Roy, A. G., & Best, J. L. (2006). Dynamics of a river channel confluence with discordant beds: Flow turbulence, bed load sediment transport, and bed morphology. Journal of Geophysical Research, 111(F4). doi: 10.1029/2005jf000458.

Bradbrook, K. F., Biron, P. M., Lane, S. N., Richards, K. S., & Roy, A. G. (1998). Investigation of controls on secondary circulation in a simple confluence geometry using a three-dimensional numerical model. Hydrological Processes, 12(8), 1371-1396. doi: 10.1002/(sici)1099-1085(19980630)12:83.0.co;2-c.

Bunte, K., Abt, S.R. (2001): Sampling surface and subsurface particle size distributions in wadable gravel- and cobble-bed streams for analysis in sediment transport, hydraulics, and streambed monitoring. U.S. Dep. of Agric., For. Serv., Rocky Mt. Res. Stn., Fort Collins, Colorado, USA.Gen. Tech. Rep. RMRS-GTR-74, 428p.

Chow, V.T. (1959). Open Channel Hydraulics. McGraw-Hill, New York.

Delacre, M., Leys, C., Mora, Y., Lakens, D. (2019). Taking Parametric Assumptions Seriously: Arguments for the Use of Welch's F-test instead of the Classical F-test in One-Way ANOVA. International Review of Social Psychology, 32(1), 13, 1-12. doi: 10.5334/irsp.19.

De Serres, B., Roy, A., Biron, P., & Best, J. L. (1999). Three-dimensional flow structure at a river channel confluence with discordant beds. Geomorphology, 26, 313-335. doi: 10.1016/S0169-555X(98)00064-6.

Dunn, O. J. (1964). Multiple comparisons using rank sums. *Technometrics*, *6*(3), 241–252. doi: 10.1080/00401706.1964.10490181

https://doi.org/10.5194/egusphere-2023-2432
Preprint. Discussion started: 13 December 2023

Embleton-Hamann, C. (1997). Geomorphological Hazards in Austria. Geomorphological Hazards of Europe, 1st ed., Vol. 1, 33-56. Elsevier Science Amsterdam, NL.

Ferguson, R., & Hoey, T. (2008). Effects of Tributaries on Main-Channel Geomorphology. River Confluences, Tributaries and the Fluvial Network (eds S.P. Rice, A.G. Roy and B.L. Rhoads), 183-206. John Wiley & Sons Hoboken, New Jersey.

Gems, B., Sturm, M., Vogl, A., Weber, C., & Aufleger , M. (2014). Analysis of Damage Causing Hazard Processes on a Torrent Fan – Scale Model Tests of the Schnannerbach Torrent Channel and its Entry to the Receiving Water. Conference Proceedings of Interpraevent 2014 in the Pacific Rim, Nara.

Gems, B., Kammerlander, J., Aufleger, M., Moser, M. (2020): Fluviatile Feststoffereignisse. In: T. Glade, M. Mergili, K. Sattler (Eds.), ExtremA 2019. Aktueller Wissensstand zu Extremereignissen alpiner Naturgefahren in Österreich. Vienna University Press, 287-321.

Guillén-Ludeña, S., Franca, M. J., Cardoso, A. H., & Schleiss, A. J. (2015). Hydro-morphodynamic evolution in a 90° movable bed discordant confluence with low discharge ratio. Earth Surface Processes and Landforms, 40(14), 1927-1938. doi: 10.1002/esp.3770.

Guillén-Ludeña, S., Cheng, Z., Constantinescu, G., & Franca, M. J. (2017). Hydrodynamics of mountain-river confluences and its relationship to sediment transport. Journal of Geophysical Research: Earth Surface, 122(4), 901-924. doi: 10.1002/2016jf004122.

Hanus, S., Hrachowitz, M., Zekollari, H., Schoups, G., Vizcaino, M., Kaitna, R. (2021): Future changes in annual, seasonal and monthly runoff signatures in contrasting Alpine catchments in Austria. Hydrology and Earth System Sciences, 25, 3429-3453. doi: 10.5194/hess-25-3429-2021

Hübl, J., & Moser, M. (2006). Risk management in Lattenbach: A case study from Austria. WIT Transactions on Ecology and the Environment, 90, 333-342. doi: 10.2495/deb060321.

https://doi.org/10.5194/egusphere-2023-2432
Preprint. Discussion started: 13 December 2023

Kammerlander, J., Gems, B., Sturm, M., & Aufleger, M. (2016). Analysis of Flood Related Processes at Confluences of Steep Tributary Channels and Their Respective Receiving Streams - 2d Numerical Modelling Application. Conference Proceedings of Interpraevent 2016, 319-326.

Keiler, M., Knight, J., & Harrison, S. (2010). Climate change and geomorphological hazards in the Eastern European Alps. Philosophical Transactions of the Royal Society A: Mathematical, Physical and Engineering Sciences, 368(1919), 2461–2479. doi: 10.1098/rsta.2010.0047

Knight, J., & Harrison, S. (2009). Sediments and future climate. *Nature Geoscience*, *2*(4), 230–230. doi: 10.1038/ngeo491

Leite Ribeiro, M., Blanckaert, K., Roy, A. G., & Schleiss, A. J. (2012a). Hydromorphological implications of local tributary widening for River Rehabilitation. Water Resources Research, 48(10), 201-217. doi: 10.1029/2011wr011296.

Leite Ribeiro, M., Blanckaert, K., Roy, A. G., & Schleiss, A. J. (2012b). Flow and sediment dynamics in channel confluences. Journal of Geophysical Research: Earth Surface, 117, F01035-. doi: 10.1029/2011jf002171.

Liu, T., Fan, B., & Lu, J. (2015). Sediment-flow interactions at channel confluences: A flume study. Advances in Mechanical Engineering, 7(6), 1-9. doi: 10.1177/1687814015590525.

Löschner, L., Herrnegger, M., Apperl, B., Senoner, T., Seher, W., Nachtnebel, H.P. (2017) Flood risk, climate change and settlement development: a micro-scale assessment of Austrian municipalities. Reg Environ Change 17, 311–322. doi: 10.1007/s10113-016-1009-0

Massey, F. J. (1951). The Kolmogorov-Smirnov test for goodness of fit. Journal of the American Statistical Association, 46(253), 68-78. doi: 10.1080/01621459.1951.10500769.

Maxwell, S. E., & Delaney, H. D. (2004). Designing experiments and analyzing data (2nd ed.). Erlbaum, Mahwah, New Jersey.

McKnight, P.E. & Najab, J. (2010). Mann-Whitney U Test. In The Corsini Encyclopedia of Psychology (eds I.B. Weiner and W.E. Craighead). doi: 10.1002/9780470479216.corpsy0524

https://doi.org/10.5194/egusphere-2023-2432
Preprint. Discussion started: 13 December 2023

Meunier, M. (1991). Eléments d'hydraulique torrentielle (Elements of torrential hydraulics). Études du Cemagref,série montagne n° 1, Cemagref, France. Available at: https://www.quae-open.com/extract/198 (in French), accessed in February 2023.

Miller, J. P. (1958). High mountain streams: Effects of geology of channel characteristics and bed material, Memoir. Bureau of Mines and Mineral Resources, Socorro, N. M.

Moder, K. (2010). Alternatives to F-test in one-way ANOVA in case of heterogeneity of variances (a simulation study). Psychological Test and Assessment Modeling, 52(4), 343-353.

Mosley, M. P. (1976). An experimental study of channel confluences. The Journal of Geology, 84(5), 535-562. doi: 10.1086/628230.

Mueller, E. R., & Pitlick, J. (2005). Morphologically based model of bed load transport capacity in a headwater stream. Journal of Geophysical Research, 110(F2). doi: 10.1029/2003jf000117.

Prenner, D., Hrachowitz, M., & Kaitna, R. (2019). Trigger characteristics of torrential flows from high to low alpine regions in Austria. Science of The Total Environment, 658, 958-972. doi: 10.1016/j.scitotenv.2018.12.206.

Rhoads, B. & Kenworthy, S. (1995). Flow structure at an asymmetrical confluence. Geomorphology, 11, 273-293. doi: 10.1016/0169-555X(94)00069-4.

Rice, S. (1998). Which tributaries disrupt downstream fining along gravel-bed rivers? Geomorphology, 22(1), 39 - 56. doi: 10.1016/s0169-555x(97)00052-4.

Roca, M., Martín-Vide, J.P., & Martin-Moreta, P. (2009). Modelling a torrential event in a river confluence. Journal of Hydrology, 364, 207-215. doi: 10.1016/j.jhydrol.2008.10.020.

Rom, J., Haas, F., Hofmeister, F., Fleischer, F., Altmann, M., Pfeiffer, M., Heckmann, T., & Becht, M. (2023). Analysing the large-scale debris flow event in July 2022 in Horlachtal, Austria, using remote sensing and measurement data. Geosciences, 13(4), 100. doi: 10.3390/geosciences13040100.

https://doi.org/10.5194/egusphere-2023-2432
Preprint. Discussion started: 13 December 2023

Roy, A., & Bergeron, N. (1990). Flow and particle paths at a natural river confluence with coarse bed material. Geomorphology, 3(2), 99-112. doi: 10.1016/0169-555x(90)90039-s.

Ruxton, G. D., & Beauchamp, G. (2008). Time for some a priori thinking about post hoc testing. Behavioral Ecology, 19/3, 690-693. doi: 10.1093/beheco/arn020.

Sawyer, S. (2009). Analysis of Variance: The Fundamental Concepts. Journal of Manual & Manipulative Therapy, 17, 27E-38E. doi: 10.1179/jmt.2009.17.2.27E.

Steinskog, D. J., Tjøstheim, D. B., & Kvamstø, N. G. (2007). A cautionary note on the use of the Kolmogorov–Simonov test for normality. Monthly Weather Review, 135(3), 1151-1157. doi: 10.1175/mwr3326.1.

Stevenson, K. J. (2011). Review of OriginPro 8.5. Journal of the American Chemical Society, 133(14), 5621-5621. doi: 10.1021/ja202216h.

Stoffel, M. (2010). Magnitude–frequency relationships of debris flows — a case study based on field surveys and tree-ring records. Geomorphology, 116(1–2), 67–76. doi: 10.1016/j.geomorph.2009.10.009.

Stoffel, M., & Huggel, C. (2012). Effects of climate change on mass movements in mountain environments. Progress in Physical Geography: Earth and Environment, 36(3), 421–439. doi: 10.1177/0309133312441010

St. Pierre Ostrander, T., Holzner, J., Mazzorana, B., Gorfer, M., Andreoli, A., Comiti, F., & Gems, B. (2023). Confluence morphodynamics in Mountain Rivers in response to intense tributary bedload input. Earth Surface Processes and Landforms, 2023, 1-22. doi: 10.1002/esp.5613.

Sturm, M., Gems, B., Keller, F., Mazzorana, B., Fuchs, S., Papathoma-Köhle, M. & Aufleger, M. (2018). Experimental analyses of impact forces on buildings exposed to fluvial hazards. Journal of Hydrology, 565, 1-13. doi: 10.1016/j.jhydrol.2018.07.070.

https://doi.org/10.5194/egusphere-2023-2432
Preprint. Discussion started: 13 December 2023

Trevisani, S., Cavalli, M., & Marchi, L. (2010). Reading the bed morphology of a mountain stream: A geomorphometric study on high-resolution topographic data. Hydrology and Earth System Sciences, 14(2), 393-405. https://doi.org/10.5194/hess-14-393-2010.

Wang, X. K., Wang, X., Lu, W., & Liu, T. (2007). Experimental study on flow behavior at open channel confluences. Frontiers of Architecture and Civil Engineering in China, 1, 211-216. doi: 10.1007/s11709-007-0025-z.

Welch, B. L. (1947). The generalization of 'student's' problem when several different population variances are involved. *Biometrika*, *34* (1–2), 28–35 doi: 10.1093/biomet/34.1-2.28

Witte, R. S., & Witte, J. S. (2017). Statistics 11th Edition. Wiley and Sons, Hoboken, New Jersey.